

DOE/NASA/0163-2
NASA CR-165128
AESD-TME-3052

Mod-0A 200 kW Wind Turbine Generator Design and Analysis Report

NATIONAL RENEWABLE ENERGY LABORATORY
LIBRARY

APR 8 - 1996

GOLDEN, COLORADO 80401-3393

T. S. Andersen, C. A. Bodenschatz,
A. G. Eggers, P. S. Hughes, R. F. Lampe,
M. H. Lipner, and J. R. Schornhorst
Westinghouse Electric Corporation
Advanced Energy Systems Division
P. O. Box 10864
Pittsburgh, Pennsylvania 15236

August 1980

Prepared for
National Aeronautics and Space Administration
Lewis Research Center
Cleveland, Ohio 44135
Under Contract DEN 3-163

for
U.S. DEPARTMENT OF ENERGY
Conservation and Solar Energy
Office of Solar Power Applications
Washington, D.C. 20545
Under Interagency Agreement DE-AB29-76ET20370

TABLE OF CONTENTS

<u>Section</u>	<u>Page</u>
Acknowledgments	ii
Table of Contents	iii
List of Figures	ix
List of Tables	xvii
Abbreviations and Acronyms	xix
SUMMARY	1
INTRODUCTION	2
CONCLUSIONS	6
 1.0 PROJECT REQUIREMENTS AND APPROACH	7
1.1 Project Requirements	7
1.2 Approach	9
1.2.1 Management of Project and Detailed Approach	9
1.2.2 Site Selection	11
1.2.3 Project Responsibilities	15
 2.0 SYSTEM DESCRIPTION	19
2.1 Features and Characteristics	19
2.2 Configuration	20
2.3 Nacelle Arrangement	20
2.4 Rotor	20
2.5 Pitch Change Mechanism	23
2.6 Pitch Hydraulic System	23
2.7 Yaw Mechanism and Brake	23
2.8 Tower and Foundation	25
2.9 Electrical Power System	25
2.10 Control Systems	29
2.11 Instrumentation and Data Acquisition	32
2.12 Predicted Performance	32
2.13 Cost	36
2.14 Weight Summary	37
 3.0 SYSTEM DESIGN REQUIREMENTS AND SPECIFICATIONS	39
3.1 System Design Requirements	39
3.2 System Specifications	48
 4.0 DESIGN AND ANALYSIS	61
4.1 Rotor and Pitch Change Mechanism	61
4.1.1 Blades	62
4.1.1.1 Requirements	62
4.1.1.2 Approach	67
4.1.1.3 Selected Design	68
4.1.1.4 Supporting Analytical Results	77
4.1.2 Hub	79
4.1.2.1 Requirements	82
4.1.2.2 Approach	82

TABLE OF CONTENTS (Cont'd)

<u>Section</u>	<u>Page</u>
4.1.2.3 Selected Design	82
4.1.2.4 Supporting Analytical Results	86
4.1.3 Pitch Change Mechanism and Hydraulic System	86
4.1.3.1 Requirements	87
4.1.3.2 Design Approach	87
4.1.3.3 Selected Design	89
4.2 Drive Train	92
4.2.1 Low Speed Shaft, Bearings and Coupling	92
4.2.1.1 Requirements	92
4.2.1.2 Design Approach	94
4.2.1.3 Selected Design	96
4.2.2 Speed Increaser	99
4.2.2.1 Requirements	99
4.2.2.2 Design Approach	102
4.2.2.3 Selected Design	102
4.2.2.4 Analytical Results	103
4.2.3 High Speed Shaft, Bearings, Couplings, Belt Drive, and Fluid Coupling	103
4.2.3.1 Requirements	103
4.2.3.2 Design Approach	106
4.2.3.3 Selected Design	106
4.2.3.4 Analytical Results	109
4.2.4 Rotor Brake	111
4.2.4.1 Requirements	111
4.2.4.2 Design Approach	111
4.2.4.3 Selected Design	112
4.2.4.4 Analytical Results	112
4.3 Nacelle Equipment	112
4.3.1 Requirements	112
4.3.2 Design Approach	113
4.3.3 Selected Design	113
4.4 Yaw Drive	117
4.4.1 Yaw Drive Mechanism	117
4.4.1.1 Requirements	117
4.4.1.2 Design Approach	118
4.4.1.3 Selected Design	118
4.4.1.4 Analytical Results	119
4.4.2 Yaw Brake	124
4.4.2.1 Requirements	124
4.4.2.2 Design Approach	124
4.4.2.3 Selected Design	124
4.5 Tower and Foundation	126
4.5.1 Tower	126
4.5.1.1 Requirements	126
4.5.1.2 Approach	127
4.5.1.3 Selected Design	128
4.5.1.4 Supporting Analytical Results	135

TABLE OF CONTENTS (Cont'd)

<u>Section</u>	<u>Page</u>
4.5.2 Foundation	138
4.5.2.1 Requirements	138
4.5.2.2 Approach	140
4.5.2.3 Selected Design	140
4.5.2.4 Supporting Analytical Results	145
4.5.3 Service Stand	148
4.5.3.1 Requirements	148
4.5.3.2 Design Approach	148
4.5.3.3 Selected Design	148
4.5.4 Equipment and Personnel Hoist	149
4.5.4.1 Requirements	149
4.5.4.2 Design Approach	149
4.5.4.3 Selected Design	149
4.6 Electrical System and Components	153
4.6.1 Generator	153
4.6.1.1 Generator Requirements	153
4.6.1.2 Approach	153
4.6.1.3 Selected Design	153
4.6.1.4 Supporting Analytical Results	156
4.6.2 Switchgear	156
4.6.2.1 Switchgear Requirements	156
4.6.2.2 Approach	161
4.6.2.3 Selected Design	161
4.6.2.4 Supporting Analytical Results	164
4.6.3 Transformer and Utility Connection	165
4.6.3.1 Requirements	165
4.6.3.2 Approach	165
4.6.3.3 Selected Design	165
4.6.4 Slip Rings	169
4.6.4.1 Requirements	169
4.6.4.2 Approach	169
4.6.4.3 Selected Design	170
4.7 Control Systems	170
4.7.1 Blade Pitch Control	170
4.7.1.1 Requirements	170
4.7.1.2 Approach	172
4.7.1.3 Selected Design	172
4.7.1.4 Supporting Analytical Results	174
4.7.2 Yaw Control	174
4.7.2.1 Requirements	174
4.7.2.2 Approach	175
4.7.2.3 Selected Design	175
4.7.2.4 Supporting Analytical Results	176
4.7.3 Generator Control	177
4.7.3.1 Requirements	177
4.7.3.2 Approach	178
4.7.3.3 Selected Design	178

TABLE OF CONTENTS (Cont'd)

<u>Section</u>	<u>Page</u>
4.7.4 Safety System	180
4.7.4.1 Requirements	180
4.7.4.2 Approach	180
4.7.4.3 Selected Design	181
4.7.5 Manual Control	183
4.7.5.1 Requirements	183
4.7.5.2 Approach	183
4.7.5.3 Selected Design	183
4.7.6 Automatic Control	184
4.7.6.1 Requirements	184
4.7.6.2 Approach	185
4.7.6.3 Selected Design	185
4.7.6.4 Supporting Analytical Results	187
4.7.7 Remote Control and Monitoring	187
4.7.7.1 Requirements	187
4.7.7.2 Approach	188
4.7.7.3 Selected Design	188
4.7.8 Control Building	188
4.7.8.1 Requirements	188
4.8 Systems Analysis	190
4.8.1 Dynamic Loads	190
4.8.2 Fatigue	201
4.8.2.1 Blades	215
4.8.2.2 Low Speed Shaft	217
4.8.2.3 Low Speed Shaft Bearings and Caps	217
4.8.2.4 Bedplate	218
4.8.2.5 Yaw Drive System	218
4.8.2.6 Tower	219
5.0 SYSTEM TESTS AND INSTALLATION	221
5.1 In Plant Tests	222
5.1.1 Drive Train and Nacelle Equipment	224
5.1.2 Rotor	228
5.1.3 Pitch Change Mechanism	232
5.1.4 System Checkout	237
5.2 Site Tests and Installation	243
5.2.1 Rotor	244
5.2.2 Systems Checkout	245
5.2.3 Drive Train and Nacelle Equipment	248
5.2.4 Installation Experience	249
6.0 SAFETY CONSIDERATIONS	253
6.1 Safety Philosophy	253
6.2 Site Description and Evaluation	253
6.3 Design Criteria	254
6.3.1 Design Requirements	254

TABLE OF CONTENTS (Cont'd)

<u>Section</u>			<u>Page</u>
	6.3.2 Compliance with Standards and Regulations	254	
	6.3.3 Site Safety.	254	
6.4	Normal and Emergency Operating Procedures	254	
6.5	Identification of Hazards	255	
	6.5.1 Obvious Hazards.	255	
	6.5.2 Safety Committee Concerns.	256	
6.6	Probability of Occurrence and Predicted Consequences . . .	256	
6.7	Safety Related Physical Design Features and Administrative Controls	259	
	6.7.1 Physical Features.	259	
	6.7.2 Administrative Controls.	261	
	6.7.2.1 Safety Committee.	261	
	6.7.2.2 Quality Assurance Procedures.	261	
6.8	Analysis of Potential Accidents	261	
6.9	Conclusions	263	
7.0	FAILURE MODES AND EFFECTS ANALYSIS	265	
7.1	Introduction.	265	
7.2	Evaluation Criteria	265	
7.3	Task Approach	265	
7.4	Summary and Conclusions	265	
8.0	ENGINEERING DATA ACQUISITION	267	
8.1	Instrumentation	267	
	8.1.1 Rotor.	267	
	8.1.2 Drive Train.	269	
	8.1.3 Nacelle/Bedplate	269	
	8.1.4 Tower.	269	
	8.1.5 Control Building (Switchgear).	275	
	8.1.6 Meteorological Tower	275	
8.2	Remote Multiplexer Units.	277	
	8.2.1 Hub RMU.	277	
	8.2.2 Bedplate RMU	277	
	8.2.3 Control Building RMU	281	
8.3	Mobile Data System	281	
8.4	Stand Alone Instrument Recorder	286	
9.0	INITIAL OPERATING PERFORMANCE	289	
9.1	Aerodynamic Performance	289	
	9.1.1 Measured Power Versus Wind Speed	289	
	9.1.2 Drive Train Efficiency	294	
	9.1.3 Cyclic Power	297	
9.2	Structural Performance.	297	
	9.2.1 Mean and Cyclic Loads.	297	
	9.2.2 Tower Shadow and Wind Shear Effects.	301	

TABLE OF CONTENTS (Cont'd)

<u>Section</u>	<u>Page</u>
9.3 Control System Performance	301
9.3.1 Yaw Control	301
9.3.2 Pitch Control	301
9.3.3 Microprocessor Control	303
9.4 Utility Interface	305
9.4.1 Voltage Variations	306
9.4.2 Frequency Variations	306
9.5 Ice Detector for Blades	309
10.0 REFERENCES AND BIBLIOGRAPHY	313
10.1 References	313
10.2 Bibliography	319
APPENDIX A: List of Engineering Drawings for the MOD-0A Wind Turbine Including the Westinghouse and NASA Lewis Research Center Drawing Numbers	321
APPENDIX B: Site Safety	353
APPENDIX C: MOD-0A Wind Turbine Generator Program Listing	365

LIST OF FIGURES

<u>Figure No.</u>	<u>Title</u>	<u>Page</u>
0-1	MOD-0A 200 kW Wind Turbine Generator; Clayton, New Mexico	5
1.2.1-1	Comparison of MOD-0 and MOD-0A Output Power as a Function of Wind Speed	10
1.2.2-1	The 17 Candidate Wind Turbine Sites	14
1.2.2-2	Aerial View of Clayton, NM with MOD-0A 200 kW Wind Turbine	16
1.2.2-3	Overall View of Clayton MOD-0A Wind Turbine Site	16
2.2-1	200-Kilowatt Wind Turbine	21
2.3-1	Nacelle Arrangement for MOD-0A Wind Turbine Generator	22
2.5-1	Blade Pitch Change Mechanism	24
2.6-1	Pitch Hydraulic System Schematic (Simplified)	24
2.7-1	Yaw Drive System	26
2.7-2	Yaw Brake System	27
2.9-1	Simplified One-Line Diagram of the Electrical Power Distribution System	28
2.10-1	Control System Interfaces	30
2.11-1	Mobile Data System Overview	33
2.12-1	Power Output as a Function of Wind Speed	34
2.12-2	MOD-0A 200 kW Wind Turbine Power Control-Output Power and Blade Pitch Angle vs. Wind Speed	35
2.12-3	Annual Energy Output for 200 kW Wind Turbine	36
4.1.1-1	MOD-0A Nacelle Final Assembly	63
4.1.1-2	MOD-0A Wind Turbine Blade Non-Destructive Testing - LAS Ontario, California	64

LIST OF FIGURES (Cont'd)

Figure No.	Title	Page
4.1.1-3	MOD-0A Blade Configuration - Planform	66
4.1.1-4	MOD-0A Wind Turbine Blade Geometry	69
4.1.1-5	Blade Chord Distribution	70
4.1.1-6	Blade Thickness Distribution	70
4.1.1-7	Blade Setting Angle B (Twist)	71
4.1.1-8	MOD-0A Blade Typical Cross Section	72
4.1.1-9	MOD-0A Blade Fastener Detail A	73
4.1.1-10	MOD-0A Blade Root End Details	74
4.1.1-11	Blade Fixture Jig Showing Length, Twist and Contour Check Points	75
4.1.1-11-A	Blade Fixture Jig Showing Length, Twist and Contour Check Points	76
4.1.1-12	Predicted Cyclic Flapwise Bending Loads for MOD-0A Blades	80
4.1.1-13	Predicted Cyclic Chordwise Bending Loads for MOD-0A Metal Blades	80
4.1.2-1	Hub After Final Machining	83
4.1.2-2	Hub and Pitch Change Mechanism After Assembly at NASA LeRC	84
4.1.2-3	Hub and Pitch Change Assembly	85
4.1.3-1	Operational Requirements of Pitch Change Mechanism	88
4.1.3-2	Pitch Change Mechanism Mounted on Hub	90
4.1.3-3	Pitch Change Mechanism (Simplified)	91
4.1.3-4	Pitch Hydraulic System Rotating Hydraulic Union	93
4.2.1-1	Cyclic Bending Moment on MOD-0A Low Speed Shaft (Calculated)	95

LIST OF FIGURES (Cont'd)

Figure No.	Title	Page
4.2.1-2	Low Speed Shaft, Bearings, Bearing Housings, and Couplings	97
4.2.1-3	Low Speed Shaft	98
4.2.2-1	Speed Increaser Installed	104
4.2.3-1	Arrangement of High Speed Shaft Components	105
4.2.3-2	Fluid Coupling, Speed Increaser, and Rotor Brake	107
4.2.3-3	Belt Drive for Generator (Shown During Belt Tension Test)	108
4.2.3-4	Effect of Fluid Coupling Slip on Relative Rotation and Drive Train Fundamental Frequency (100 kW, Synchronized)	110
4.3-1	Bedplate, Support Cone, Mounting Frame, Service Stand, and Yaw System	115
4.3-2	Nacelle	116
4.4-1	Effect of Brake Pressure on Restraining Yaw Moment	120
4.4-2	Yaw Torque Vs. Rotation for Several Preload Torques	121
4.4-3	Turntable Bearing and Gear Assembly	125
4.5-1	Nacelle Assembly Installation on Tower	129
4.5.1-1	Original MOD-0 Tower with Service Stairs and Equipment Rails	130
4.5.1-2	MOD-0A Tower During Trial Assembly at Manufacturer (Side View)	131
4.5.1-3	MOD-0A Tower During Trial Assembly at Manufacturer (Bottom View)	132
4.5.1-4	MOD-0A Tower Round Pipes and Welded Joints	133

LIST OF FIGURES (Cont'd)

Figure No.	Title	Page
4.5.1-5	MOD-OA Tower Gussets, Bolted Joints, Channels in Lower Section of Tower	134
4.5.1-6	MOD-OA Fully Assembled	136
4.5.1-7	Tower Hurricane Load Plus Deadweight	137
4.5.2-1	MOD-OA Wind Turbine	139
4.5.2-2	MOD-OA Mat Foundation (Forms still in place)	141
4.5.2-3	Completed Mat with Control Building Base	142
4.5.2-4	Mat Reinforcing Rods (Before concrete was poured)	143
4.5.2-5	Tower Leg Mount on Completed Foundation . .	144
4.5.2-6	Design Loading Data (for foundation)	146
4.5.2-7	Wind Turbine Tower Foundation Load Schematic	147
4.5.4-1	Equipment and Personnel Hoist	150
4.6.1-1	MOD-OA Generator	154
4.6.1-2	MOD-OA Generator	155
4.6.2-1	MOD-OA Power System One-Line Diagram	158
4.6.2-2	MOD-OA Switchgear	159
4.6.3-1	MOD-OA Oil Circuit Recloser	167
4.6.3-2	MOD-OA Transclosure Housing	168
4.6.4-1	MOD-OA Rotor Slip Ring	171
4.7-1	MOD-OA Control System Interfaces	172
4.7.1-1	Block Diagram of Blade Pitch Control in the Power Control Mode with Wind Feed Forward	174

LIST OF FIGURES (Cont'd)		
Figure No.	Title	Page
4.7.2-1	MOD-OA Yaw Control Block Diagram	175
4.7.2-2	Yaw Angle Error	177
4.7.3-1	Generator Control Elementary	179
4.7.4-1	Safety System Block Diagram	181
4.7.7-1	Remote Control and Monitoring System	189
4.8.1-1	Blade Coupled Frequency Spectrum Cantilever Mode	192
4.8.1-2	Blade Loads Case 1 ~ Mean Loads	194
4.8.1-3	Blade Loads Case 2 ~ Mean Loads	195
4.8.1-4	Blade Loads Case 3 ~ Mean Loads	196
4.8.1-5	Blade Loads Case 4 ~ Mean Loads	197
4.8.1-6	Blade Loads Case 1, 2, and 4 ~ Cyclic Loads	198
4.8.1-7	Blade Loads Case 3 ~ Cyclic Loads	199
4.8.1-8	Blade Centrifugal Force	200
4.8.1-9	Cyclic Flapwise Bending Loads in MOD-0 Blades Before and After Wind Turbine Modifications	202
4.8.1-10	Cyclic Chordwise Bending Loads in MOD-0 Blades Before and After Wind Turbine Modifications	203
4.8.2-1	Substructures and Interfaces for Fatigue Analysis of MOD-OA WTG	214
4.8.2-2	Result of Fatigue Analysis of MOD-OA Blade Assuming Structure Quality Comparable to Airplane Wing Structure . . .	216
4.8.2-3	Result of Fatigue Analysis of MOD-OA Blade Indicating Life Predictions as S/S_0 and K_T Vary	216

LIST OF FIGURES (Cont'd)

Figure No.	Title	Page
5-1	Flow Chart for Assembly of MOD-0A WTG at NASA Lewis Research Center	223
5-2	Flow Chart for of MOD-0A WTG at Clayton, N.M.	223
5.1.1-1	Sketch of Setup for In Plant Testing of the Drive Train Assembly	224
5.1.1-2	Photograph of In Plant Test Setup for Drive Train Assembly	226
5.1.1-3	Temperature of Oil in Speed Increaser As a Function of Time for Drive Train Tests	227
5.1.2-1A	Photograph of Loading Fixture and Test Setup Used During Strain Gage Calibrations (Side View)	229
5.1.2-1B	Photograph of Loading Fixture and Test Setup Used during Strain Gage Calibrations (Looking Upwind)	229
5.1.2-2	Strain Gage Calibration Results for Bending Moments on the Low Speed Shaft . . .	231
5.1.2-3	Strain Gage Calibration Results for Torque Loading on the Low Speed Shaft . . .	231
5.1.3-1	Sketch of In Plant Test Setup for Phase II and III Acceptance Testing	233
5.1.3-2	Block Diagram of Pitch Control System for In Plant Tests	233
5.1.3-3	Blade Simulators Attached to Hub Assembly for Static In Plant Testing of Pitch Change Mechanism	235
5.1.3-4	Manual Pot Calibration Results for Pitch Controller	238
5.1.4-1	Service Stand, Mounting Frame, Support Cone, and Control Rack	239

Figure No.	LIST OF FIGURES (Cont'd) Title	Page
5.1.4-2	Photograph of MOD-OA WTG Assembly Prior to Phase III In Plant System Checkout Tests	239
5.2.4-1	Installation of MOD-OA Tower on Foundation at Clayton, N.M.	250
5.2.4-2	Final Stage of WTG Lifting Operation and Installation to the Tower	252
8.1-1	MOD-OA Blade Strain Gage Locations	270
8.1-2	MOD-OA Blade Strain Gage Locations	271
8.1-3	MOD-OA Blade Strain Gage Locations - Reference Centerlines	272
8.2-1	MOD-OA Remote Multiplexer Unit Number Two .	278
8.3-1	Mobile Data System	283
8.3-2	Interior of Mobile Data System (Looking forward)	284
8.3-3	Interior of Mobile Data System (Looking Aft)	285
9.1.1-1	Alternator Power Output vs. Wind Speed Measured on the Nacelle	290
9.1.1-2	Simultaneous Two-Minute Averages of Meteorological Tower Wind Speed at 100 Feet vs. Nacelle Wind Speed	291
9.1.1-3	Clayton New Mexico Power vs. Rescaled Wind at 100 Feet	292
9.1.1-4	Power Coefficient vs. Tip Speed Ratio . . .	293
9.1.2-1	Average Rotor Torque vs. Average Power for Each Revolution	295
9.1.2-2	Comparison of the Design Value of Drive Train Efficiency with Measured Values at Various Alternator Powers	296
9.1.3-1	Cyclic Power vs. Wind Speed	298

LIST OF FIGURES (Cont'd)

Figure No.	Title	Page
9.2.1-1	Mean and Cyclic Chordwise Loads at Station 40	299
9.2.1-2	Mean and Cyclic Flapwise Loads at Station 40	300
9.2.2-1	Strip Chart Records of Flapwise and Chordwise Bending Moments at Station 40 . .	302
9.3.1-1	Strip Chart Records Illustrating Typical Yaw Maneuvers	302
9.3.2-1	Rotor Speed, Blade Pitch Angle, and Alternator Power for Wind Turbine Startup	303
9.3.2-2	Rotor Speed, Blade Pitch Angle, and Alternator Power for Wind Turbine Shutdown	304
9.3.3-1	Low Wind Startup and Shutdown	305
9.4.2-1	System and Wind Turbine Frequency Characteristics - Clayton, NM.	307
9.4.2-2	Wind Speed, System Frequency and Power versus Time with Constant Winds - Clayton, NM.	309
9.4.2-3	Wind Speed and Power versus Time with Gusting and Small Frequency Excursions - Clayton, NM.	310
9.4.2-4	Wind Speed, System Frequency and Power versus Time with Gusting and Large Frequency Excursions - Clayton, NM.	311
9.5-1	Ice Shed From Blades	312

LIST OF TABLES

Table No.	Title	Page
1.2.2-1	General Characteristics of Clayton, NM (Population, Energy Consumption, Power Demand, Elevation, Mean Wind Speeds, and Temperature)	15
1.2.3-1	Project Responsibilities for the Four MOD-OA Wind Turbine Sites	17
2.13-1	MOD-OA 200 kW WTG Costs (\$K)	36
2.14-1	MOD-OA 200 kW WTG Weights	37
3.2-1	System Specifications for MOD-OA 200 kW WTG	50
4.1.1-1	MOD-OA Blade Design Requirements	65
4.1.1-2	MOD-OA Blade Loads NASA "Red Line" Bending Moments	81
4.1.1-2A	MOD-OA Blade Loads NASA "Red Line" Bending Moments	81
4.6.1-1	Generator Electrical Characteristics	157
4.8.1-1	Design Condition as Specified by Contract .	193
4.8.1-1A	Design Condition as Specified by Contract .	193
4.8.2-1	MOD-OA Fatigue Loads	204
4.8.2-1A	MOD-OA Fatigue Loads	205
4.8.2-2	MOD-OA Fatigue Loads	206
4.8.2-2A	MOD-OA Fatigue Loads	207
4.8.2-3	MOD-OA Fatigue Loads	208
4.8.2-3A	MOD-OA Fatigue Loads	209
4.8.2-4	MOD-OA Fatigue Loads	210
4.8.2-4A	MOD-OA Fatigue Loads	211
4.8.2-5	MOD-OA Fatigue Loads	212
4.8.2-5A	MOD-OA Fatigue Loads	213

LIST OF TABLES (Cont'd)

<u>Table No.</u>	<u>Title</u>	<u>Page</u>
5-1	In Plant Test of Clayton MOD-0A 200 kW WTG	221
5-2	Site Tests of Clayton MOD-0A 200 kW WTG . .	221
5-3	Installation of Clayton MOD-0A 200 kW WTG .	222
6.8-1	Results of Blade Failure Analysis	262
8.1-1	Rotor Sensors	268
8.1-2	Drive Train Sensors	273
8.1-3	Nacelle/Bedplate Sensors	274
8.1-4	Tower Sensors	274
8.1-5	Switchgear Sensors	276
8.1-6	Meteorological Tower Sensor	276
8.2-1	RMU Number One Located on the Hub	279
8.2-2	RMU Number Two Located on the Bedplate . . .	280
8.2-3	RMU Number Three Located in the Control Building	282
8.4-1	SAIR Data Tape Channels	287

4.8 SYSTEMS ANALYSIS

4.8.1 DYNAMIC LOADS

The structural design loads presented herein are for the four structural design conditions specified in Section 4.1.1.1.⁴¹ This load set is the basis on which the structural integrity of the blades was predicted. The dynamic analysis was originally performed for MOD-0, and the MOD-0A work is essentially an update. A fixed rotor axis computer program* was utilized to define, in detail, the steady state and cyclic loads acting on the windmill blades. This computer program performs a coupled response analysis that yields spanwise and azimuthal distributions of airloads, bending moments and torsional moments depending on the operational mode selected.

In brief this computer program is a fully coupled aeroelastic blade loads analysis consisting of an aerodynamic performance/trim analysis of a rotor system that is coupled with the dynamic response of the blades. A relaxation type of iterative procedure is employed between the aerodynamics and blade responses to obtain a converged solution that is consistent with the blade mode shape. The aerodynamic portion of the program consists of expressions for rotor thrust, torque, shaft moments, and shaft shear forces utilizing C_l , C_d , and C_m data versus local blade angle of attack, section thickness, and Mach number. An iterative procedure permits one or all of the net rotor forces to be trimmed to describe the operational condition of the rotor in terms of the rotor control angles and/or attitude that is consistent with the response of the blades. The dynamic analysis portion of the program considers the blade response, in harmonic form, to the steady and unsteady airloads, Coriolis forces, gravitational effects and the structural coupling between the flapwise and chordwise bending moments due to collective pitch and local geometric twist angle. The structural model utilizes a finite element description that permits a detail definition of the rotor blade system. This description is unique in that two separate beams are defined to describe one integral rotor blade. The two beams are represented as 1) the feathering blade with provisions for up to 45 stations, and 2) the fixed hub which supports the blade with provisions for up to 31 stations. A total of 44 blade stations are used to represent the windmill blades. This arrangement permits the determination and inclusion, in the net response of the blade, of 1) feather bearing radial forces, 2) feather bearing support elasticity, and 3) kick shear forces resulting from the blade retention mechanism. A quasi-coupled elastic torsion analysis is made where extensive use is made of the output from the basic coupled analysis. The elastic twist angles, as determined in the torsion analysis, are reflected in the aerodynamics of the successive aerostructure cycle in the relaxation process.

Among the many program operating options provided there is one that permits the application of an arbitrary spanwise air loading distribution to the blade structure at any discrete exciting frequency that is an integer multiple of the rotor speed. It is this option that is used to determine the aero-elastic characteristics of the blades for the specified air loads of this concept.

Rotating natural frequencies and mode shapes are computed by the program and utilize the same structural description and inputs as that employed in the

* Code developed by Lockheed

blade loads analysis. This approach ensures the computation of blade frequencies that are directly compatible with computed blade loads.

Natural frequencies for the cantilever blades were computed at various rotor speeds from zero to 50 rpm and at pitch settings, defined at the 3/4 blade radius, of 10° , 0° , and -10° . The results of these calculations for MOD-0 are presented in Figure 4.8.1-1 and show that, for the normal operating speed of 40 rpm, there is adequate separation of the blade frequencies from the aerodynamic excitations at the integer multiples of the rotor speed, nP . Also, the frequency spectrum shows that there is a negligible variation in the frequencies within the blade pitch settings investigated.

The first and lowest mode is $2.76P$ and it is defined as the first flapping mode where the primary blade motion is normal to the plane of rotation. The second mode is $3.62P$ and is defined as the first inplane mode with primary blade motions in the rotational plane. The third mode is at $7.57P$ and shows that the primary motion is again normal to the plane of rotation and it is called the second flapping mode.

The four design conditions are summarized in Table 4.8.1-1. They are described in Section 4.1.1.1 of this report.

For each of the loading cases in Table 4.8.1-1 steady and cyclic, 1P, blade loads were computed. This computation process uses the specified airloads as inputs to obtain the steady state blade bending loads and elastic characteristics. The gravitational effect, due to the spanwise blade mass distribution, is used to define the cyclic blade bending loads and elastic characteristics.

The influence of inplane Coriolis accelerations on cyclic bending loads are obtained independently and superimposed on those due to the gravitational effects. The distribution of the cyclic inplane blade root moment along the span of the blade is accomplished by using a predetermined 1P bending distribution curve. The net spanwise distribution of the cyclic chordwise bending moment is the sum of that due to gravity effects and those due to Coriolis acceleration. The spanwise distribution of the steady state beamwise and chordwise bending moments and inplane and axial shears for the four loading conditions are shown on Figures 4.8.1-2 through Figure 4.8.1-5. Figure 4.8.1-6 presents the net cyclic bending loads for cases 1, 2, and 4 and Figure 4.8.1-7 gives those for case 3. The centrifugal force distribution along the blade span for the nominal rotor speed of 40 rpm is shown on Figure 4.8.1-8.

The wind turbine blades are designed to the aeroelastic loads developed for the four original design conditions. Additional loading conditions were explored to ascertain the influence of various parameters on design loads that may affect the life and reliability of the blades and/or tower. The following conclusions were arrived at:

1. Tower shadow interference has a pronounced effect on the magnitude of cyclic blade bending moments and tower loads depending on size of blockage

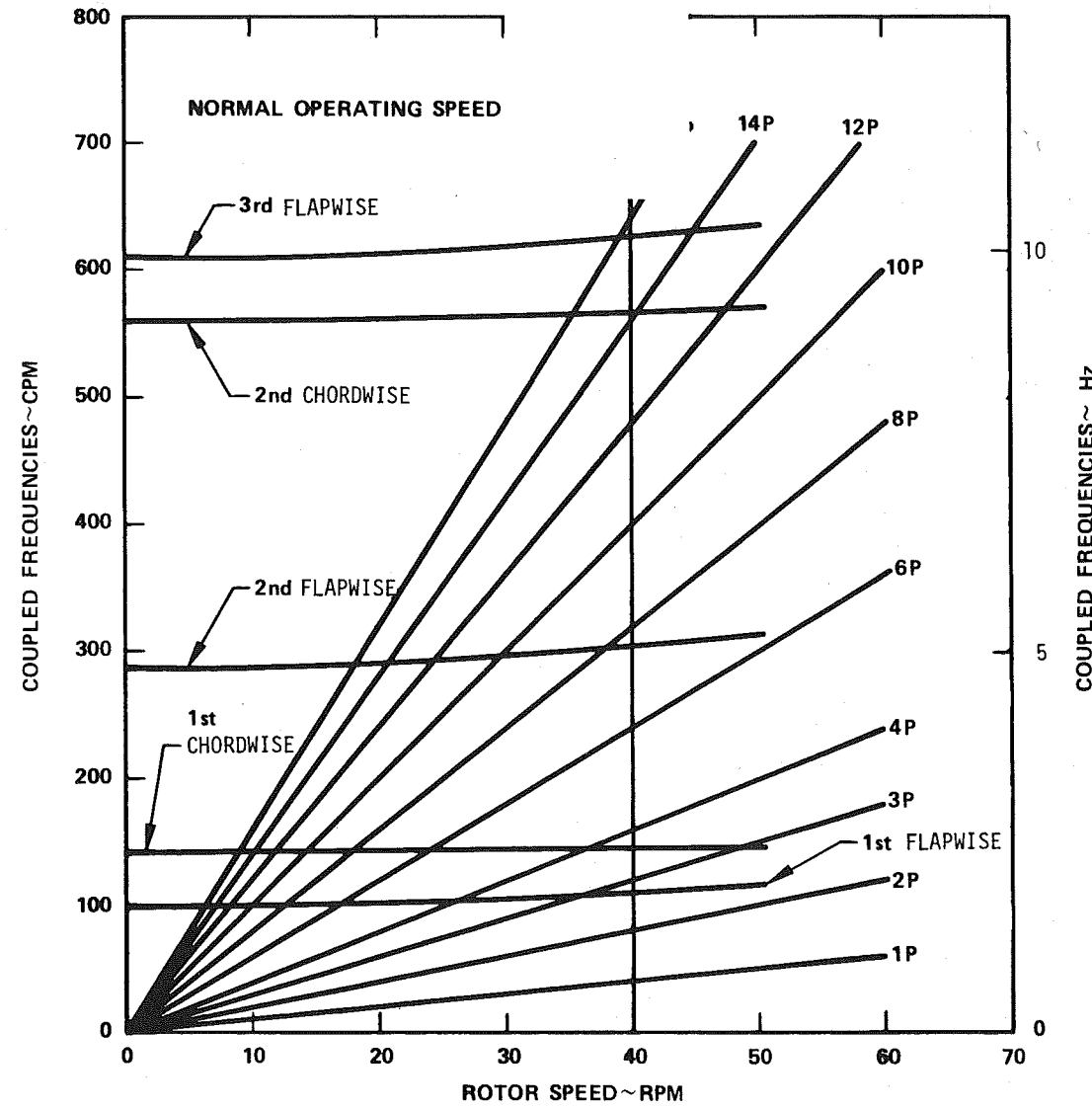


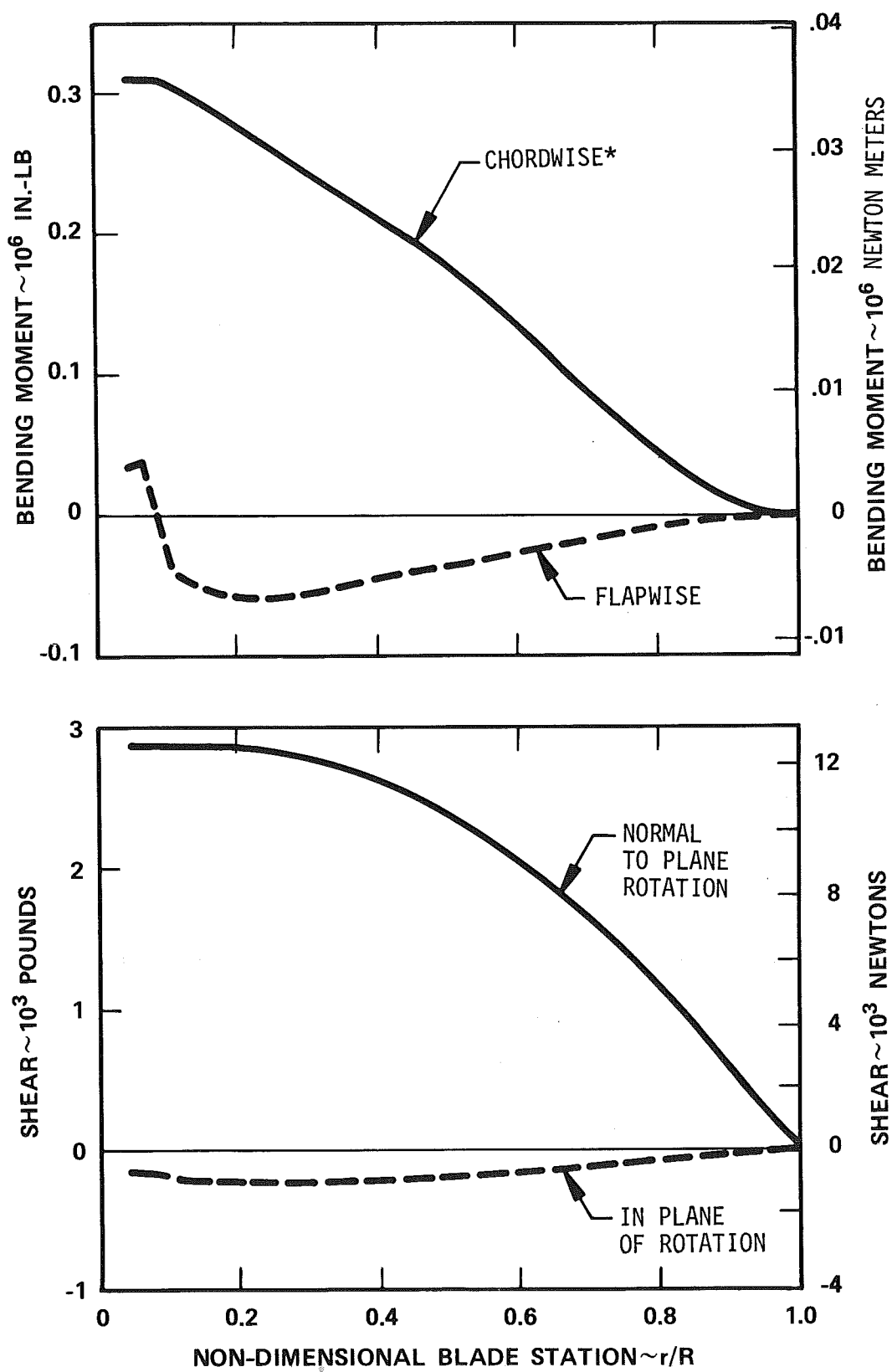
Figure 4.8.1-1. Blade Coupled Frequency Spectrum Cantilever Mode

TABLE 4.8.1-1
DESIGN CONDITION AS SPECIFIED BY CONTRACT

CASE NO.	BLADE PITCH SETTING @ 3/4 RADIUS	ROTOR SPEED rpm	WIND VELOCITY mph
1	0°	40.	18.
2	0°	40.	60.
3	-90°	40.	18.
4	0°	40.	0.

TABLE 4.8.1-1A
DESIGN CONDITION AS SPECIFIED BY CONTRACT

CASE NO.	BLADE PITCH SETTING @ 3/4 RADIUS	ROTOR SPEED rpm	WIND VELOCITY m/sec
1	0°	40.	8.0
2	0°	40.	26.8
3	-90°	40.	8.0
4	0°	40.	0.0



*MOMENT IN CHORD PLANE

Figure 4.8.1-2. Blade Loads Case 1 ~ Mean Loads

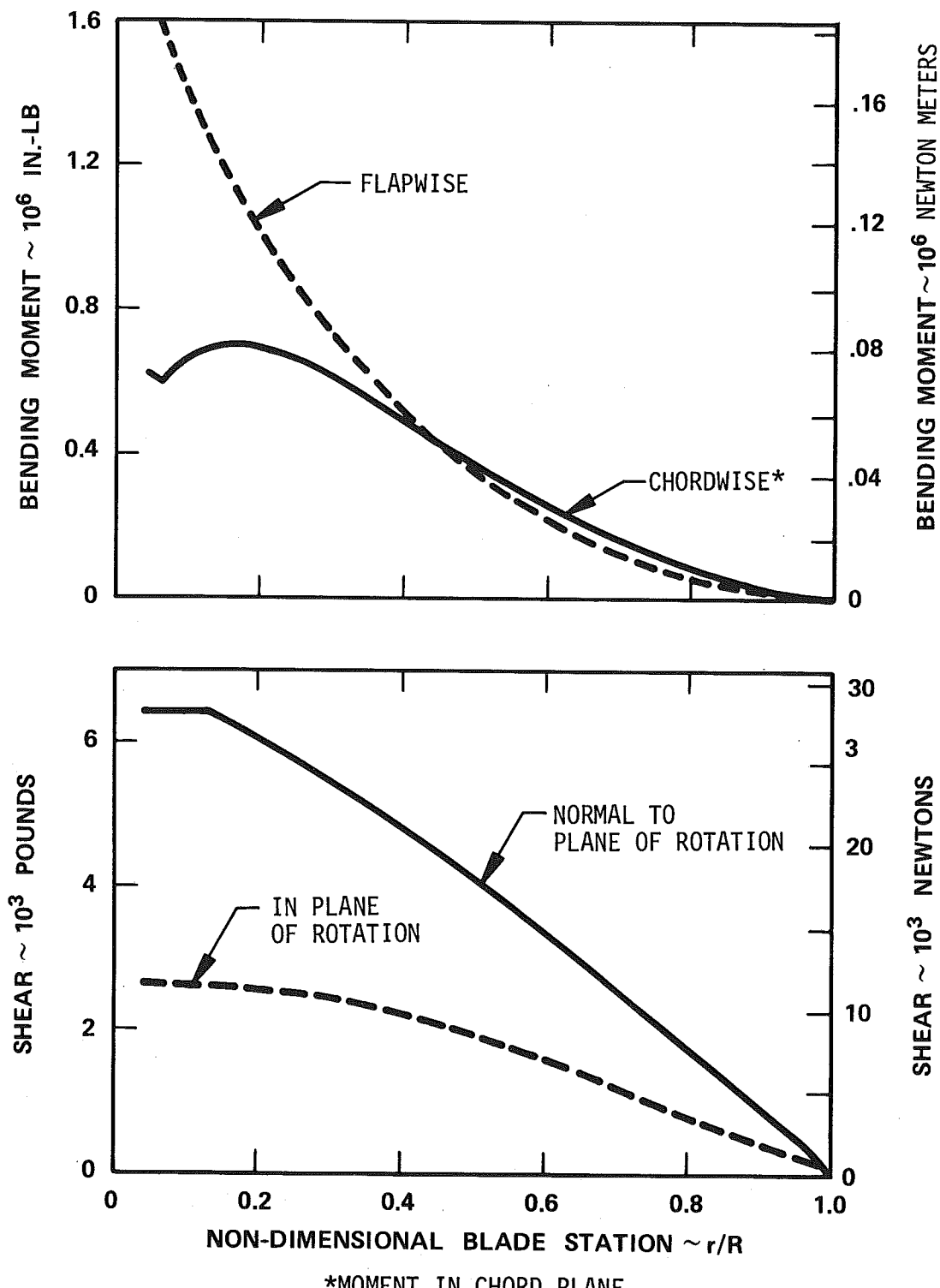


Figure 4.8.1-3. Blade Loads Case 2 ~ Mean Loads

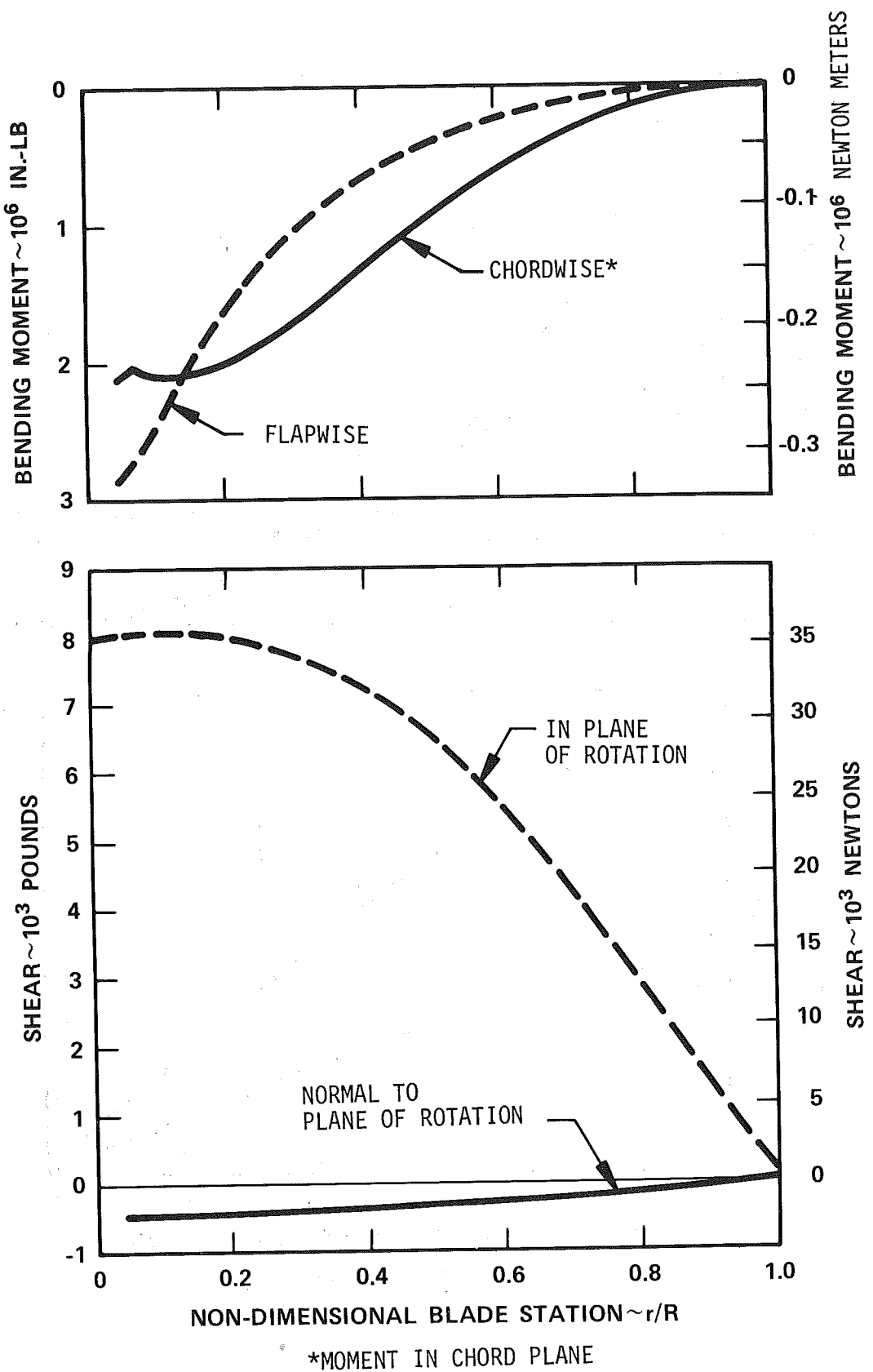


Figure 4.8.1-4. Blade Loads Case 3 ~ Mean Loads

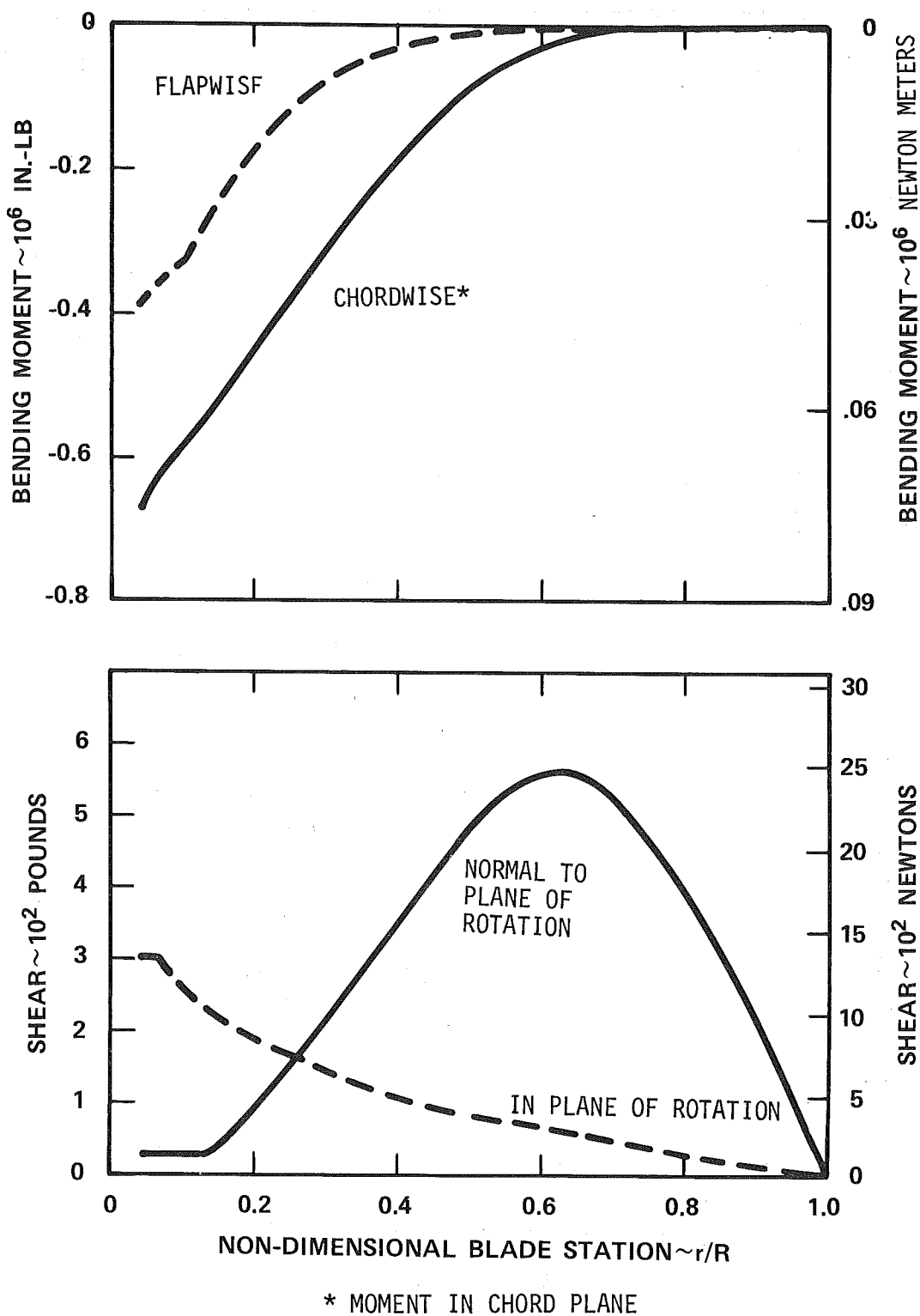


Figure 4.8.1-5. Blade Loads Case 4 ~ Mean Loads

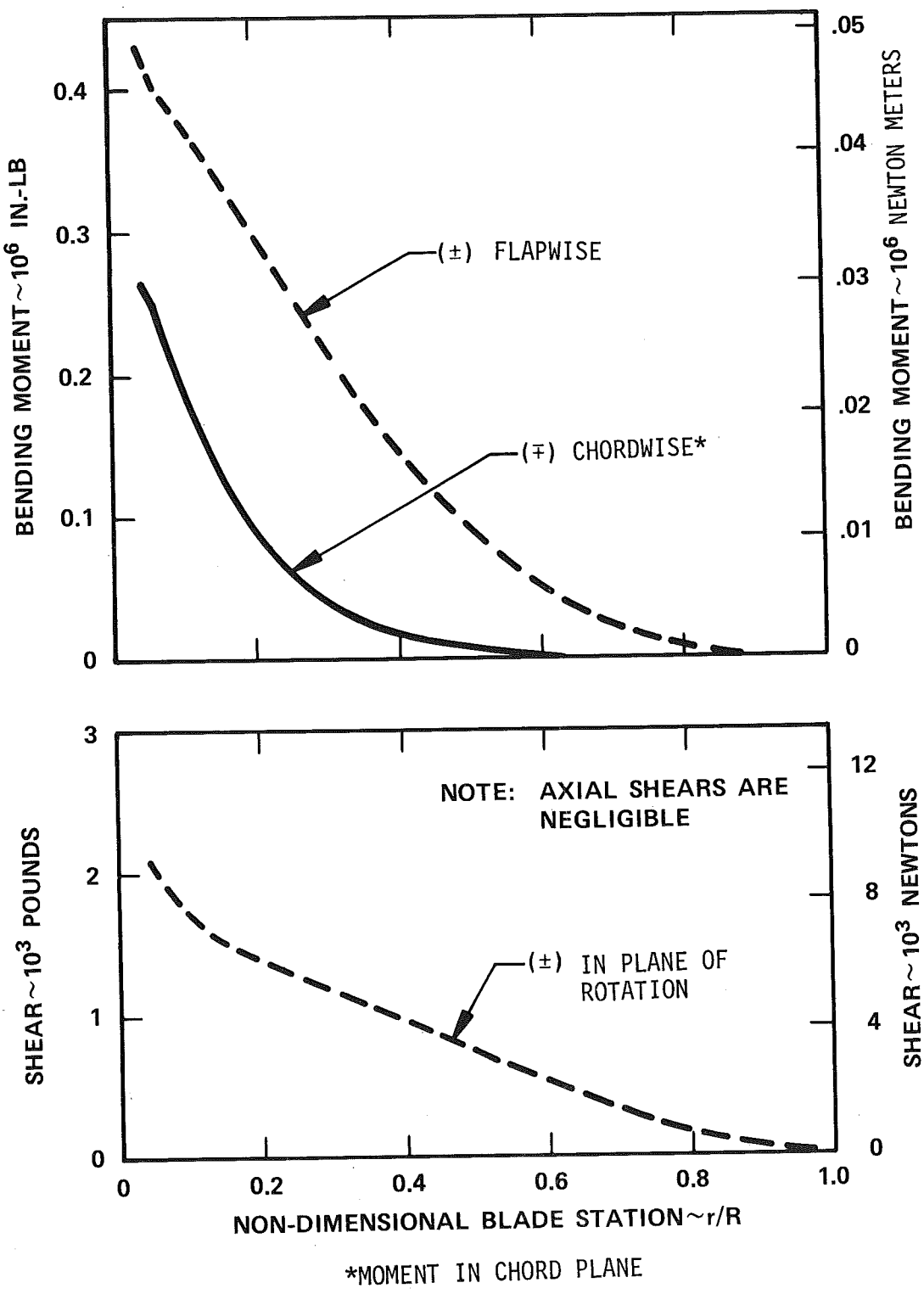


Figure 4.8.1-6. Blade Loads Case 1, 2, and 4 ~ Cyclic Loads

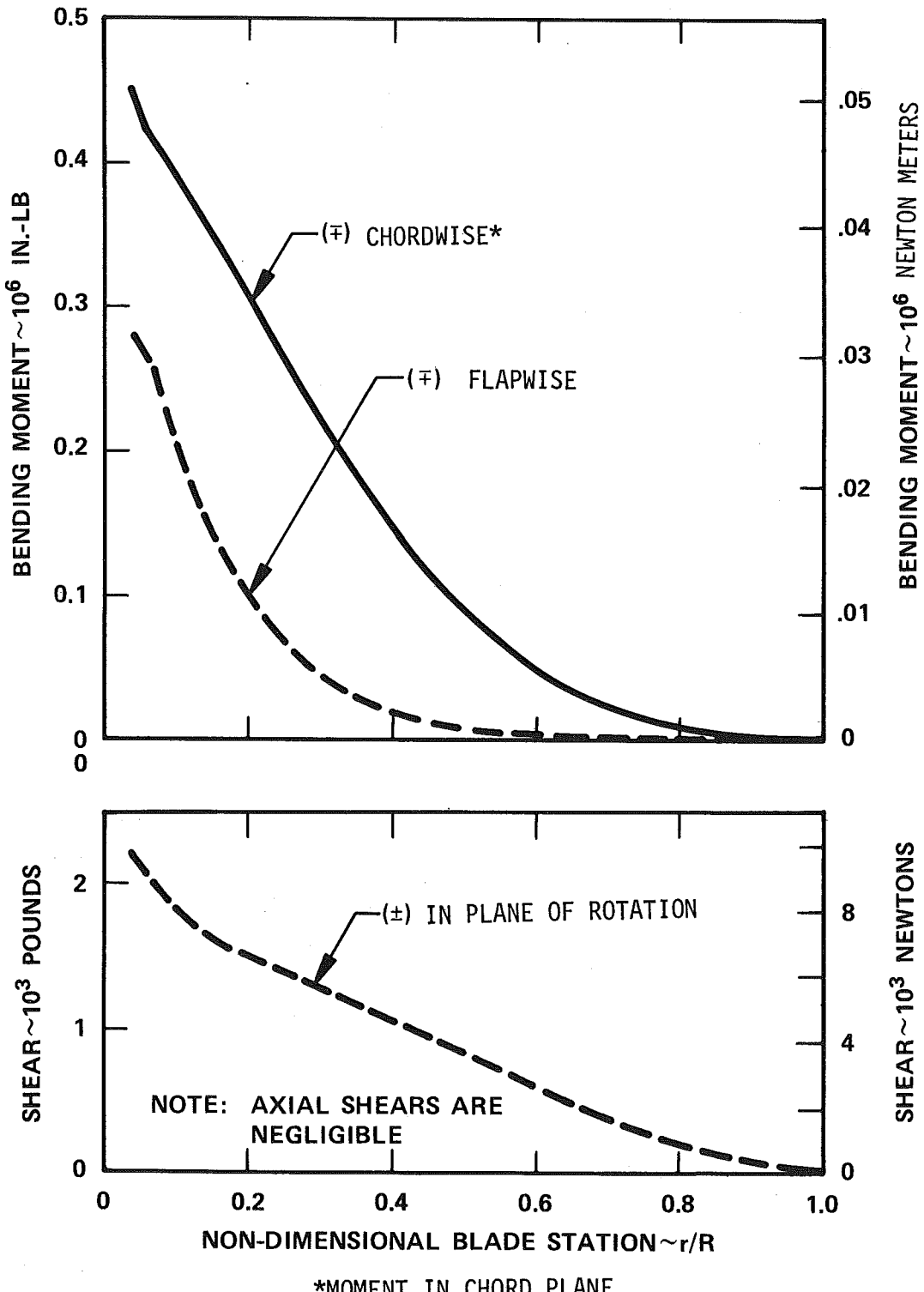


Figure 4.8.1-7. Blade Loads Case 3 ~ Cyclic Loads

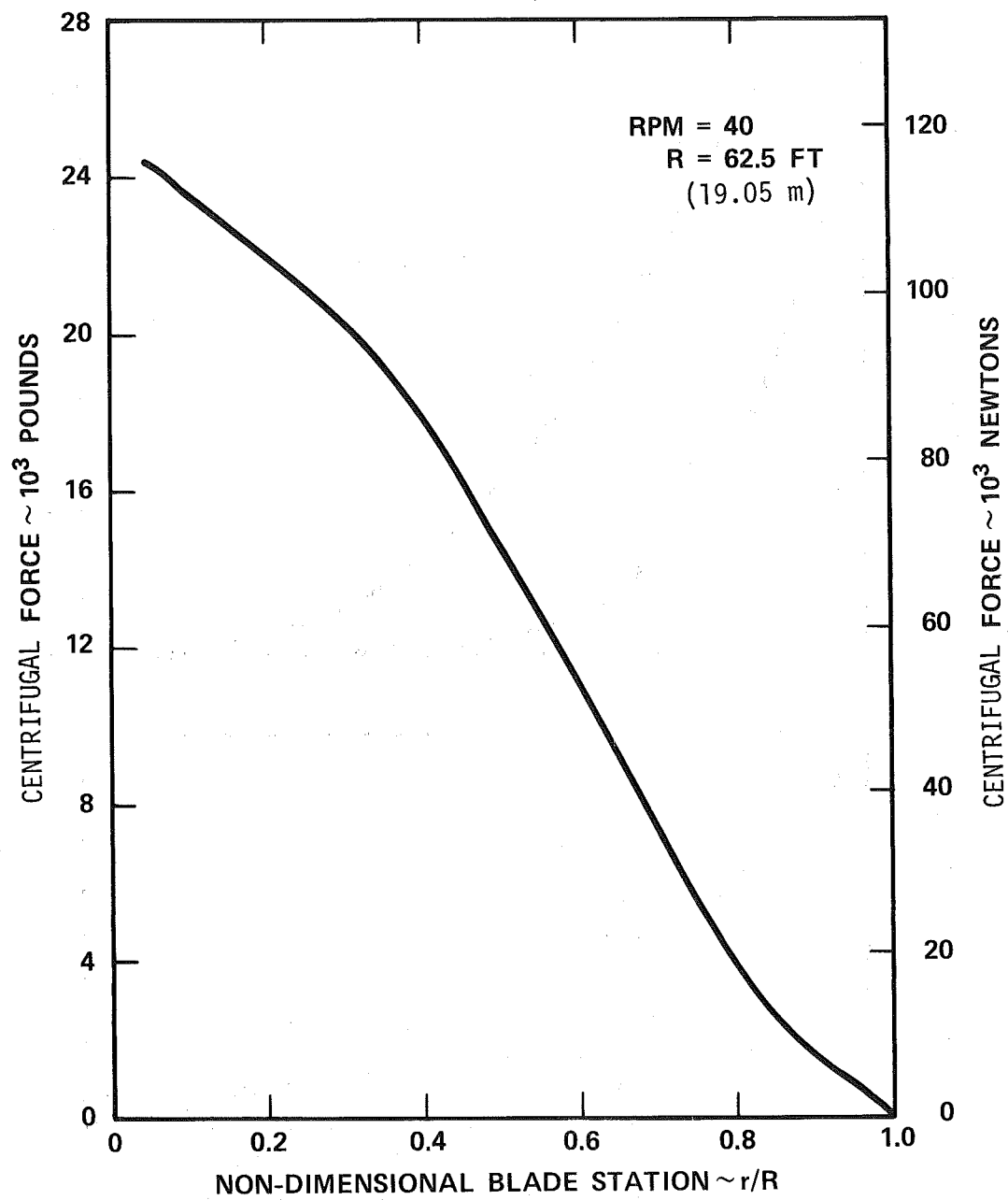


Figure 4.8.1-8. Blade Centrifugal Force

and/or the degree of free stream wind velocity retardation over the rotor sector.

2. Cyclic beamwise bending moments due to tower shadow were shown to increase the baseline cyclic moments used for fatigue analysis. The increase is most significant in the mid span. This loading should be further investigated relative to its effect on fatigue life.
3. Tower shadow tends to reduce the energy extracted from the wind, for a given blade pitch setting, resulting in a less efficient wind energy generator when compared to analysis that ignores the tower.
4. Horizontal ground wind shear results in primarily 1P blade loads and steady and 2P tower loads for a linear wind shear gradient. However, a non-linear wind shear would result in higher frequency blade and tower loads in addition to those experienced for a linear wind shear gradient. This results in larger cyclic loads and will adversely effect the wind energy system.
5. Failure of the yaw control (unable to adjust to the wind direction and/or excess yaw rates) will produce relatively large cyclic blade and tower loads affecting the life of the wind energy system.

As discussed in Section 4.1.1.4, higher loads than these predictions were encountered in MOD-0. Both tower shadow and yaw system problems were found to exist. Modifications were made to the MOD-0 to decrease the shadow and stiffen the yaw system. Figures 4.8.1-9 and 4.8.1-10 summarize the measured and predicted MOD-0 blade loads. After the tower and yaw system modifications were made, the data agreed well with predictions.

This work was updated for MOD-OA. The predicted blade loads are given in Section 4.1.1.4 in Figures 4.1.1-12 and 13. The dynamic analysis produces blade loads at two locations along the length. The detailed loading at other locations is determined from a beam analysis of the blade using the known loads at the two locations.

The loads at numerous interfaces in the WTG are tabulated in Section 4.8.2 where the fatigue analysis is documented. The loads have been computed from the rotor analysis as though the rotor axis is fixed. They have been applied statically to the nacelle and tower for the fatigue work. It has been shown that this approach is conservative.

4.8.2 FATIGUE

Loads were obtained from the WTG dynamic analysis for use in fatigue evaluation of the MOD-OA WTG. Tables 4.8.2-1 through 4.8.2-5 list the specific loads at five key system interfaces. The interface locations are shown in Figure 4.8.2-1. The blade angle listed is clockwise relative to a plumb line looking downwind. All of the fatigue loads are for the worst continuous normal operating condition; 40 mph (18.0 m/s) wind velocity while generating 200 kW of power.

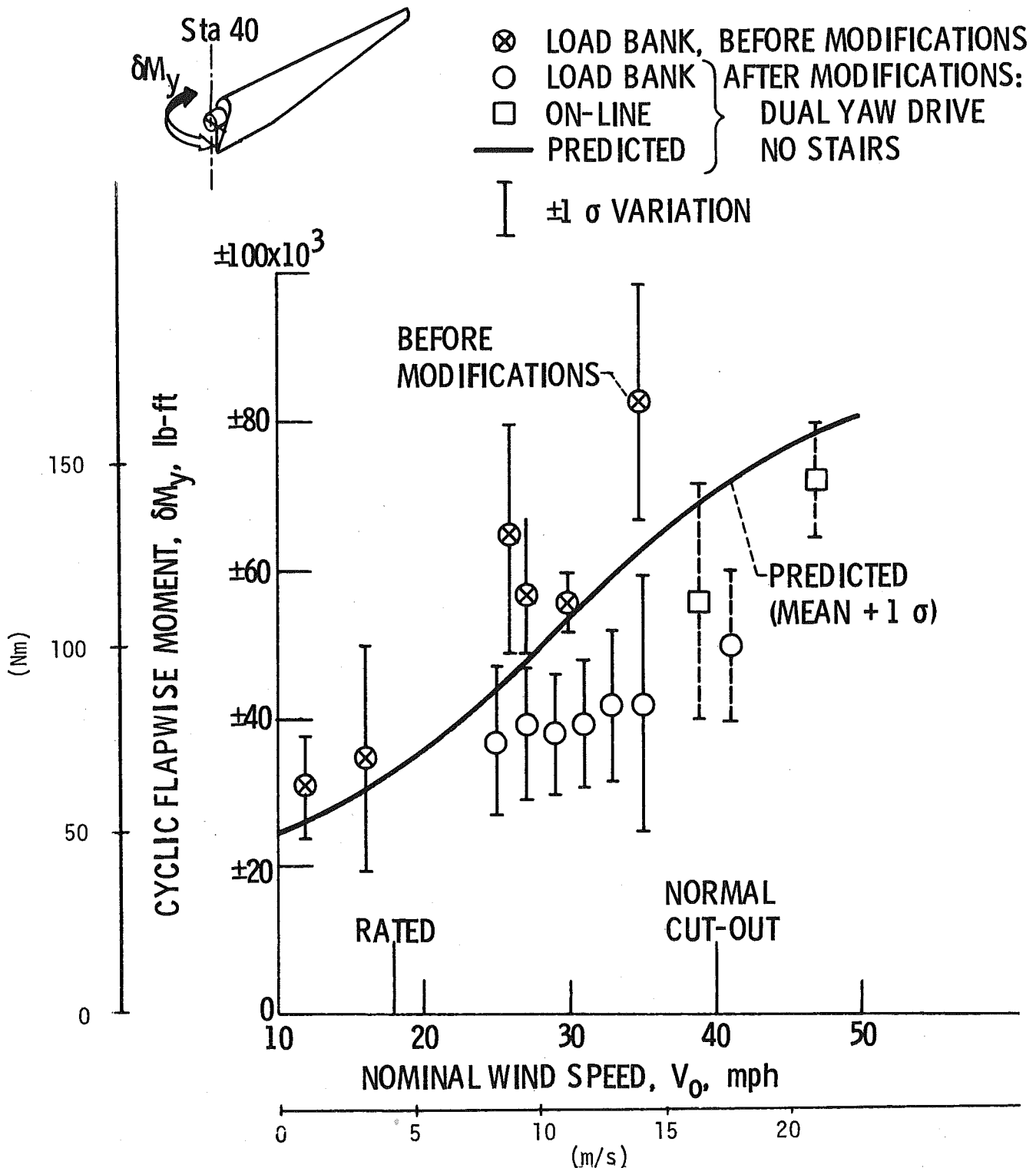


Figure 4.8.1-9 Cyclic Flapwise Bending Loads in MOD-0 Blades Before and After Wind Turbine Modifications

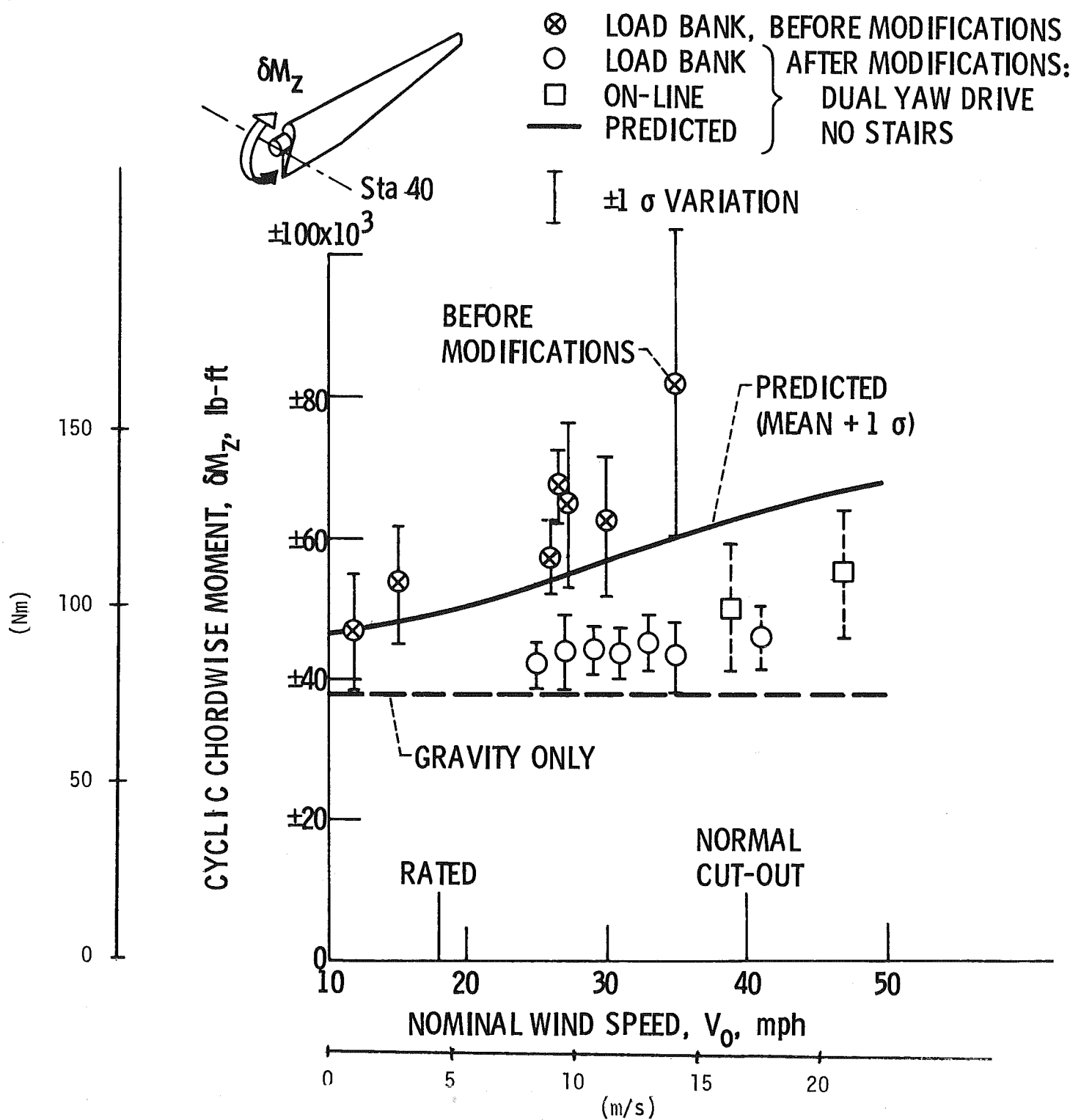


Figure 4.8.1-10 Cyclic Chordwise Bending Loads in MOD-0 Blades Before and After Wind Turbine Modifications

TABLE 4.8.2-1
MOD-OA FATIGUE LOADS
Interface 12: Hub loads on blade

BLADE AZIM., ψ_b , DEG	FORCE LOADS, lb			MOMENT LOADS, ft-lb		
	RADIAL F_x	LATERAL F_y	AXIAL F_z	RADIAL M_x	LATERAL M_y	AXIAL M_z
0	30700	-300	-3200	0	-87800	1700
15	30700	400	-3700	-900	-111300	-14400
30	30500	1000	-3800	-300	-118000	-42800
45	30100	1900	-3100	-400	-94900	-37500
60	29700	200	-2100	-200	-62800	-2900
75	29000	-700	-1400	0	-37500	18200
90	28400	400	-1000	0	-26500	-1900
105	27800	2100	-1000	-100	-26900	-36500
120	27300	2400	-1100	-100	-30600	-41200
135	26800	1000	-1100	0	-30500	-12600
150	26400	-300	-900	100	-24500	14300
165	26100	-600	-600	100	-14500	20300
180	26100	-900	-300	0	-4900	26800
195	26100	-2300	-100	0	300	54900
210	26400	-3700	-200	100	-100	84900
225	26800	-3600	-400	100	-5100	80600
240	27200	-2000	-600	0	-13000	45700
255	27800	-1000	-900	0	-21400	24800
270	28400	-2100	-1100	200	-29800	45800
285	29000	-3900	-1400	400	-37500	81200
300	29600	-4200	-1700	500	-45100	86200
315	30100	-2800	-1900	400	-52600	57300
330	30500	-1500	-2100	200	-59700	30200
345	30700	600	-2600	100	-69800	7300
Steady	28400	-900	-2000	-200	-58800	21700
Cyclic	± 2300	± 3300	± 1800	± 700	± 59200	± 64500
Freq.	1P	1P	1P	1P	1P	1P

TABLE 4.8.2-1A
MOD-OA FATIGUE LOADS
Interface 12: Hub loads on blade

BLADE AZIM., ψ_b , DEG	FORCE LOADS, N			MOMENT LOADS, N m		
	RADIAL F_x	LATERAL F_y	AXIAL F_z	RADIAL M_x	LATERAL M_y	AXIAL M_z
0	136560	-1334	-14234	0	-119040	2305
15	136560	1779	-16458	-1220	-150903	-19524
30	135671	4448	-16903	-470	-159987	-58029
45	133891	8452	-13789	-542	-128667	-50843
60	132112	890	-8896	-271	-85145	-3932
75	128998	-3114	-6228	0	-50843	24676
90	126330	1779	-4448	0	-35929	-2576
105	123661	9341	-4448	-136	-36452	-49487
120	121436	10676	-4893	-136	-41488	-55860
135	119212	4448	-4893	0	-41352	-17083
150	117433	-1334	-4003	136	-33218	19388
165	116099	-2669	-2669	136	-19660	27523
180	116099	-4003	-1334	0	-6644	36336
195	116099	-10231	-445	0	407	74434
210	117433	-16458	-890	136	-136	115108
225	119212	-16014	-1779	136	-6915	109279
240	120992	-8896	-2669	0	-17626	61961
255	123661	-4448	-4003	0	-29015	33624
270	126330	-9341	-4893	271	-40403	62096
285	128998	-17348	-6228	542	-50843	110092
300	131667	-18683	-7562	678	-61147	116872
315	133891	-12455	-8452	542	-71316	77688
330	135671	-6672	-9341	271	-80943	40946
345	1365	2669	-11565	136	-94636	9897
Steady	126330	-4003	-8896	-271	-79722	29421
Cyclic	± 10231	± 14679	± 8007	± 949	± 80264	87450
Freq.	1P	1P	1P	1P	1P	1P

TABLE 4.8.2-2
MOD-0A FATIGUE LOADS
Interface 23: Shaft Loads on hub

BLADE AZIM., ψ_b , DEG	FORCE LOADS, 1b			MOMENT LOADS, ft-1b		
	RADIAL F_x , 23	LATERAL F_y , 23	AXIAL F_z , 23	RADIAL M_x , 23	LATERAL M_y , 23	AXIAL M_z , 23
0	13000	600	3500	3800	-113300	31400
15	12700	4800	3100	15700	-143100	52100
30	11400	8800	3000	30400	-147400	48900
45	9300	11100	3500	33800	-113100	47300
60	6600	9100	4200	24100	-65300	47000
75	3400	8100	4700	18500	-23200	47200
90	0	10500	4800	26800	-3600	48200
105	-3400	13700	4500	39100	17500	49100
120	-6400	13500	4200	39100	27300	49400
135	-9100	9500	4000	25800	40200	49100
150	-11100	5200	4000	12300	58100	48800
165	-12500	2200	3800	3100	82700	30500
180	-13000	-600	3500	-3800	113300	31400
195	-12700	-4800	3100	-15700	143100	52100
210	-11400	-8800	3000	-30400	147400	48900
225	-9300	-11100	3500	-33800	113100	47300
240	-6600	-9100	4200	-24100	65300	47000
255	-3400	-8100	4700	-18500	23200	47200
270	0	-10500	4800	-26800	-3600	48200
285	3400	-13700	4500	-39100	-17500	49100
300	6400	-13500	4200	-39100	-27300	49400
315	9100	-9500	4000	-25800	-40200	49100
330	11100	-5200	4000	-12300	-58100	48800
345	12500	-2200	3800	-3100	-82700	30500
Steady	0	0	3900	0	0	41300
Cyclic	± 13000	± 13700	± 900	± 39100	± 147400	± 10800
Freq.	1P	1P	2P	1P	1P	2P

TABLE 4.8.2-2A
MOD-OA FATIGUE LOADS
Interface 23: Shaft Loads on hub

BLADE AZIM., ψ_b , DEG	FORCE LOADS, N			MOMENT LOADS, N-m		
	RADIAL $F_{x,23}$	LATERAL $F_{y,23}$	AXIAL $F_{z,23}$	RADIAL $M_{x,23}$	LATERAL $M_{y,23}$	AXIAL $M_{z,23}$
0	57827	2669	15569	5152	-153614	42573
15	56492	21351	13789	21286	-194018	70638
30	50710	39144	13345	41217	-199848	66300
45	41368	49375	15569	45827	-153343	64130
60	29358	40479	18683	32675	-88535	63723
75	15124	36031	20907	25083	-31455	63995
90	0	46706	21351	36336	-4881	65350
105	-15124	60941	20017	53012	23727	66571
120	-28469	60051	18683	53012	37014	66977
135	-40479	42258	17793	34980	54504	66571
150	-49375	23131	17793	16677	78773	66164
165	-55603	9786	16903	4203	112126	41352
180	-57827	-2669	15569	-5152	153614	42573
195	-56942	-21351	13789	-21286	194018	70638
210	-50710	-39144	13345	-41217	199848	66300
225	-41368	-49375	15569	-45827	153343	64130
240	-29358	-40479	18683	-32675	88535	63723
255	-15124	-36031	20907	-25083	31455	63995
270	0	-46706	21351	-36336	-4881	65350
285	41368	-60941	20017	-53012	-23727	66571
300	28469	-60051	18683	-53012	-37014	66977
315	40479	-42258	17793	-34980	-54504	66571
330	49375	-23131	17793	-16677	-78773	66164
345	55603	-9786	16903	-4203	-112126	41352
Steady	0	0	17348	0	0	55995
Cyclic	± 57827	± 60941	± 4003	± 53012	± 199848	± 14643
Freq.	1P	1P	2P	1P	1P	2P

TABLE 4.8.2-3
MOD-0A FATIGUE LOADS

BLADE AZIM., ψ_b , DEG	BED PLATE M_z , 34a	AXIAL MOMENT LOADS, ft-lb (ALL OTHERS ZERO)						
		GEARBOX		M_z , 47	GEN. DRIVE		BEDPLATE	
		M_z , 34a	M_z , 43b		M_z , 74	M_z , 73	M_z , 34b	M_z , 37
0	31400	-31400	32100	-710	710	-710	-32100	710
15	52100	-52100	53300	-1180	1180	-1180	-53300	1180
30	48900	-48900	50000	-1110	1110	-1110	-50000	1110
45	47300	-47300	48400	-1080	1080	-1080	-48400	1080
60	47000	-47000	48000	-1070	1070	-1070	-48000	1070
75	47200	-47200	48300	-1070	1070	-1070	-48300	1070
90	48200	-48200	49300	-1100	1100	-1100	-49300	1100
105	49100	-49100	50200	-1110	1110	-1110	-50200	1110
120	49400	-49400	50500	-1120	1120	-1120	-50500	1120
135	49100	-49100	50200	-1110	1110	-1110	-5020	1110
150	48800	-48800	49900	-1110	1110	-1110	-49900	1110
165	30500	-30500	31100	-690	690	-690	-31100	690
180								
195								
210								
225								
240								
255				REPEAT	ABOVE			
270								
285								
300								
315								
330								
345								
Steady	41300	-41300	42200	-940	940	-940	-42200	940
Cyclic	± 10800	± 10800	± 11100	± 240	± 240	± 240	± 11100	± 240
Freq.	2P	2P	2P	2P	2P	2P	2P	2P

TABLE 4.8.2-3A
MOD-OA FATIGUE LOADS

BLADE AZIM., ψ_b , DEG	BED PLATE $M_{z,34a}$	AXIAL MOMENT LOADS, N m (ALL OTHERS ZERO)						
		GEARBOX		$M_{z,47}$	GEN. DRIVE		BEDPLATE	
		$M_{z,34a}$	$M_{z,43b}$		$M_{z,74}$	$M_{z,73}$	$M_{z,34b}$	$M_{z,37}$
0	42573	-42573	43522	-963	963	-963	-43522	963
15	70638	-70638	72265	-1600	1600	-1600	-72265	1505
30	66300	-66300	67791	-1505	1505	-1505	-67791	1505
45	64130	-64130	65622	-1464	1464	-1464	-65622	1464
60	63723	-63723	65079	-1451	1451	-1451	-65079	1451
75	63995	-63995	65486	-1451	1451	-1451	-65486	1451
90	65350	-65350	66842	-1505	1505	-1505	-66842	1505
105	66571	-66571	68062	-1505	1505	-1505	-66062	1505
120	66977	-66977	68469	-1519	1519	-1519	-68469	1519
135	66571	-66571	68062	-1505	1505	-1505	-68062	1505
150	66164	-66164	67655	-1505	1505	-1505	-67655	1505
165	41352	-41352	42166	-936	936	-936	-42166	936
180	42573	-42573	43522	-963	963	-963	-43522	963
195	70638	-70638	72265	-1600	1600	-1600	-72265	1600
210	66300	-66300	67791	-1505	1505	-1505	-67791	1505
225	64130	-64130	65622	-1464	1464	-1464	-65622	1464
240	63723	-63723	65079	-1451	1451	-1451	-65079	1451
255	63995	-63995	65486	-451	1451	-1451	-65486	1451
270	65350	-65350	66842	-1505	1505	-1505	-66842	1505
285	66571	-66571	68062	-1505	1505	-1505	-68062	1505
300	66977	-66977	68469	-1519	1519	-1519	-68469	1519
315	66571	-66571	68062	-1505	1505	-1505	-68062	1505
330	66164	-66164	67655	-1505	1505	-1505	-67655	1505
345	41352	-41352	42166	-936	936	-936	-42166	936
Steady	55995	-55995	57216	-1274	1274	-1274	-57216	1274
Cyclic	± 14643	± 14643	± 15050	± 325	± 325	± 325	± 15050	325
Freq.	2P	2P	2P	2P	2P	2P	2P	2P

TABLE 4.8.2-4
MOD-0A FATIGUE LOADS
Interface 35: Yaw drive loads on bedplate

BLADE AZIM., ψ_b , DEG	FORCE LOADS, lb			MOMENT LOADS, ft-lb		
	VERTICAL F_x , 35	LATERAL F_y , 35	AXIAL F_z , 35	VERTICAL M_x , 35	LATERAL M_y , 35	AXIAL M_z , 35
0	40000	600	3500	9400	-242399	33500
15	40500	1300	3100	-8700	-275300	49600
30	41300	1900	3000	-28600	-282800	55800
45	41400	1300	3500	-42900	-247100	52200
60	38200	-1100	4200	-55900	-167500	42800
75	35700	-1200	4700	-29400	-123800	42900
90	37500	0	4800	3600	-125300	48200
105	41100	-300	4500	3800	-186400	48000
120	41900	-1200	4200	-7900	-197900	45000
135	40100	-300	4000	7100	-178700	48000
150	39300	1000	4000	28700	-179800	52600
165	39700	1200	3800	30000	-207400	34000
180						
195						
210						
225						
240						
255				REPEAT ABOVE		
270						
285						
300						
315						
330						
345						
Steady	38800	400	3900	-13000	-203300	44600
Cyclic	+3100	+1600	+900	+43000	+79500	+11200
Freq.	2P	2P	2P	2P	2P	2P

TABLE 4.8.2-4A
 MOD-OA FATIGUE LOADS
 Interface 35: Yaw drive loads on bedplate

BLADE AZIM., ψ_b , DEG	FORCE LOADS, N			MOMENT LOADS, N-m		
	VERTICAL F_x , 35	LATERAL F_y , 35	AXIAL F_z , 35	VERTICAL M_x , 35	LATERAL M_y , 35	AXIAL M_z , 35
0	177929	2669	15569	12745	-328649	45420
15	180153	5783	13789	-11796	-373257	67249
30	183712	8452	13345	-38776	-383425	75655
45	184156	5783	15569	-58165	-335023	70774
60	169922	4893	18683	-75790	-227100	58029
75	158802	-5338	20907	-39861	-167850	58165
90	166808	0	21351	4881	-169884	65350
105	182822	-1334	20017	5152	-252724	65079
120	186381	-5338	18683	-10711	-268316	61012
135	178374	-1334	17793	9626	-242285	65079
150	174815	4448	17793	38912	-243776	71316
165	176594	5338	16903	40675	-281197	46098
180	177929	2669	15569	12745	-328649	45420
195	180153	5783	13789	-11796	-373257	67249
210	183712	8452	13345	-38776	-383425	75655
225	184156	5783	15569	-58165	-335023	70774
240	169922	4893	18683	-75790	-227100	58029
255	158802	-5338	20907	-39861	-167850	58165
270	166808	0	21351	4881	-169884	65350
285	182822	-1334	20017	5152	-252724	65079
300	186381	-5338	18683	-10711	-268316	61012
315	178374	-1334	17793	9626	-242285	65079
330	174815	4448	17793	38912	-243776	71316
345	176594	5338	16903	40675	-281197	46098
Steady	172591	1779	17348	-17626	-275638	60469
Cyclic	±13789	±7117	±4003	±58300	±107788	±15185
Freq.	2P	2P	2P	2P	2P	2P

TABLE 4.8.2-5
MOD-0A FATIGUE LOADS
Interface 56: Tower loads on yaw drive

BLADE AZIM. ψ , DEG	FORCE LOADS, 1b			MOMENT LOADS, ft-1b		
	VERTICAL F_x , 56	LATERAL F_y , 56	AXIAL F_z , 56	VERTICAL M_x , 56	LATERAL M_y , 56	AXIAL M_z , 56
0	41000	600	3500	9400	-254300	35400
15	41500	1300	3100	-8700	-286000	54100
30	42300	1900	3000	-28600	-293100	62200
45	42400	1300	3500	-42900	-259100	56700
60	39200	-1100	4200	-55900	-182000	38900
75	36700	-1200	4700	-29400	-129900	38900
90	38500	0	4800	3600	-151600	48200
105	42100	-300	4500	3800	-201800	47000
120	42900	-1200	4200	-7900	-212300	41900
135	41100	300	4000	7100	-192300	47900
150	40300	-1000	4000	28700	-193300	56100
165	40700	-1200	3800	30000	-220500	38800
180						
195						
210						
225						
240						
255				REPEAT ABOVE		
270						
285						
300						
315						
330						
345						
Steady	39800	400	3900	-1300	-211500	48800
Cyclic	± 3100	± 1600	± 900	± 43000	± 81600	± 13400
Freq.	2P	2P	2P	2P	2P	2P

TABLE 4.8.2-5A
 MOD-0A FATIGUE LOADS
 Interface 56: Tower loads on yaw drive

BLADE AZIM., ψ , DEG	FORCE LOADS, N			MOMENT LOADS, N m		
	VERTICAL F_x , 56	LATERAL F_y , 56	AXIAL F_z , 56	VERTICAL M_x , 56	LATERAL M_y , 56	AXIAL M_z , 56
0	182377	2669	15569	12745	-344785	47996
15	184601	5783	13789	-11796	-387764	73350
30	188160	8452	13345	-38776	-397390	84332
45	188605	5783	15569	-58165	-351292	76875
60	174370	4893	18683	-75790	-246759	52741
75	163250	-5338	20907	-39861	-176121	52741
90	171257	0	21351	4881	-205542	65350
105	187270	-1334	20017	5152	-273604	63723
120	190829	-5338	18683	-10711	-287840	56809
135	182822	-1334	17793	9626	-260724	64944
150	179263	4448	17793	38912	-262080	76061
165	181043	5338	16903	40675	-298958	52606
180	182377	2669	15569	12745	-344785	47996
195	184601	5783	13789	-11796	-387764	73350
210	188160	8452	13345	-38776	-397390	84332
225	188605	5783	15569	-58165	-351292	76875
240	174370	4893	18683	-75790	-246759	52741
255	163250	-5338	20907	-39861	-176121	52741
270	171257	0	21351	4881	-205542	65350
285	187270	-1334	20017	5152	-273604	63723
300	190829	-5338	18683	-10711	-287840	56809
315	182822	-1334	17793	9626	-260724	64944
330	179263	4448	17793	38912	-262080	76061
345	181043	5338	16903	40675	-298958	52606
Steady	177039	1779	17348	-17626	286756	66164
Cyclic	± 13789	± 7117	± 4003	± 58300	± 110635	± 18168
Freq.	2P	2P	2P	2P	2P	2P

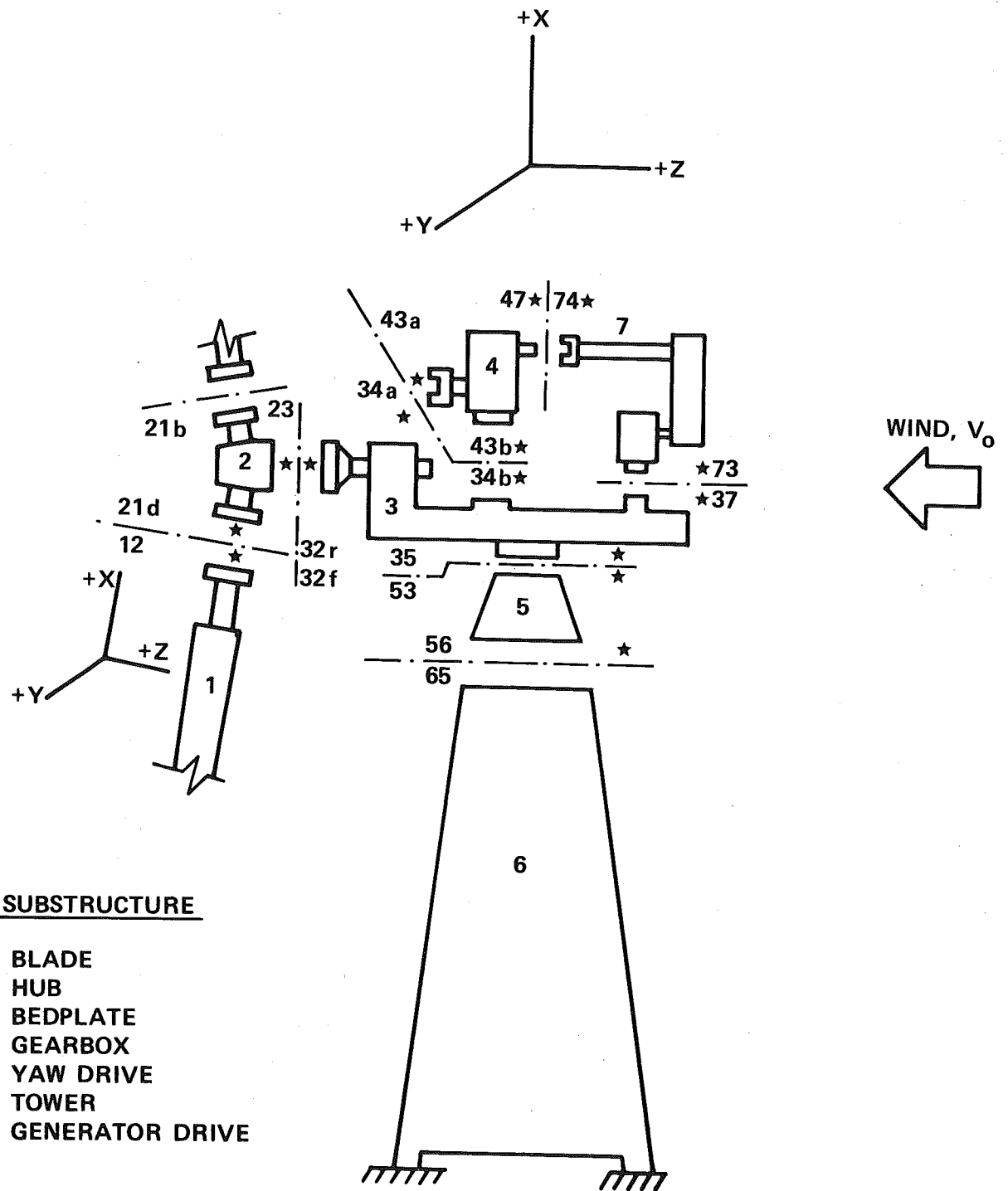


Figure 4.8.2-1. Substructures and Interfaces for Fatigue Analysis of MOD-0A WTG

4.8.2.1 BLADES

Blade fatigue life prediction entails many uncertainties. For example, there are many situations that might cause the blade loads to exceed the design values, and untested structural details can cause concern regarding blade life prediction even under known load conditions. The curve in Figures 4.8.2-2 shows the results of a fatigue analysis that was made for the MOD-0A blade structure.⁵¹ The analysis assumed:

- Blade station 637.5 is most critical.
- Load distributions as specified above apply.
- The wind turbine will operate at speeds up to the cut-off wind speed for 50 percent of the time.
- The quality of structure (design and manufacture) is comparable to that of an airplane wing, i.e., stress concentrations exist at some local structural details.

The prediction does not consider effects of fretting, corrosion, or other unpredictable damage. The figure shows that a life of 30 years should be attainable with a cut-off wind speed of 41 mph (18.3 m/s).

Many other load reversals can accumulate to damage the structure even though any one separately considered situation would produce loads that fall within ultimate strength limits. Operating conditions that cause load reversals that can accumulate to adversely affect fatigue are:

- Combinations of yaw angle, yaw rates, wind direction, and wind speed;
- Rotor speed and blade pitch setting variations which may cause unanticipated load changes.
- A large number of start-stop cycles
- Nonrotating loads during very high winds.
- Load reversals due to varying amount of tower-flow-through blockage.
- Fluctuations of electrical load demand.
- Frequent actuation of emergency systems.

Results of the fatigue analysis were also plotted (Figure 4.8.2-3) to show what might be expected if

- Loads or stresses are different from those calculated, and/or
- the quality of the structure is different from that expected.

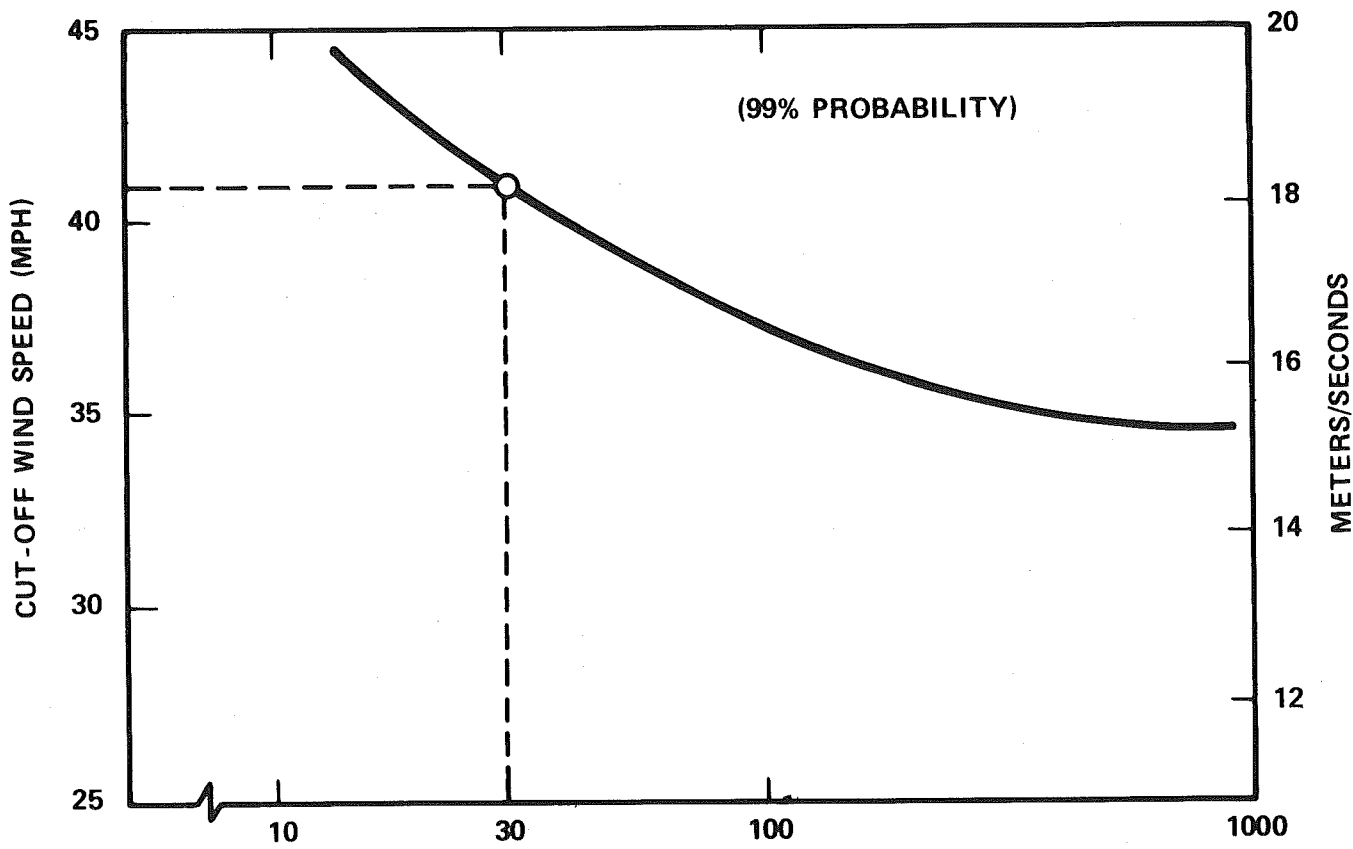


Figure 4.8.2-2. Result of Fatigue Analysis of MOD-0A Blade Assuming Structure Quality Comparable to Airplane Wing Structure

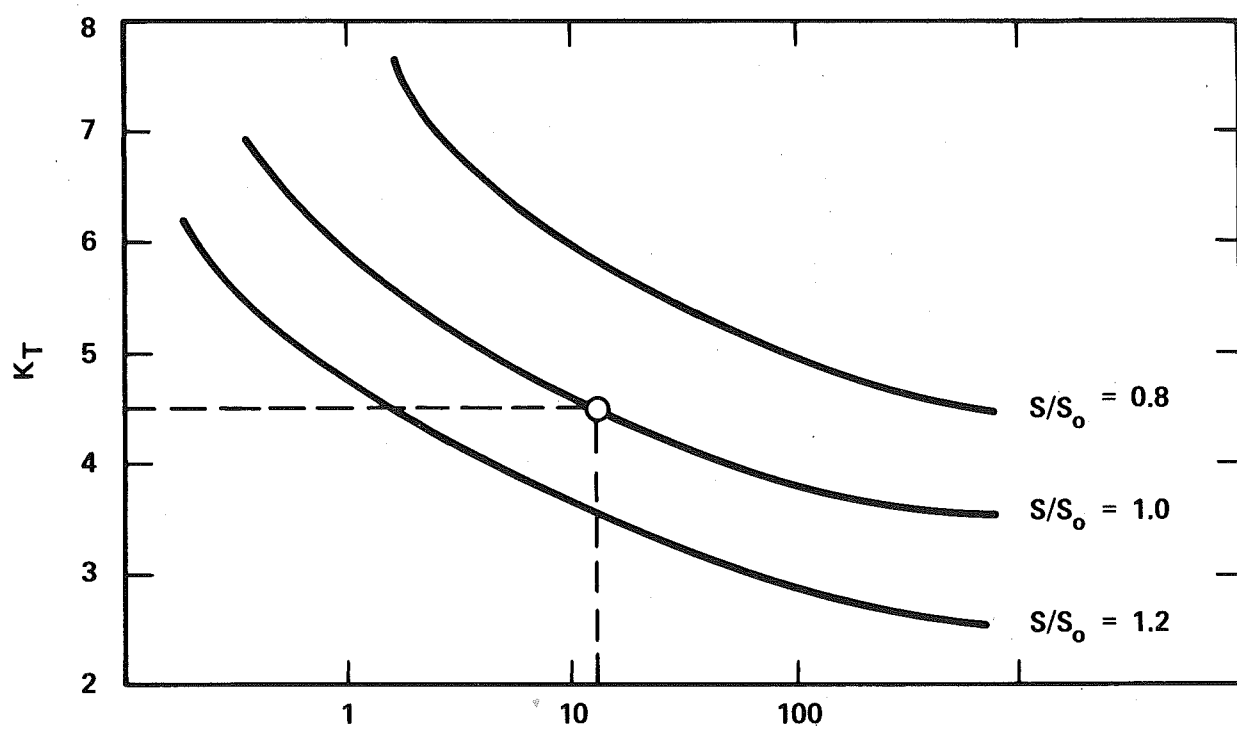


Figure 4.8.2-3. Result of Fatigue Analysis of MOD-0A Blade Indicating Life Predictions as S/S_o and K_T Vary

Interpretation of Figure 4.8.2-3 requires definition of two symbols which are common to fatigue analysis, S/S_0 and K_T . S represents stress, and the subscript, o , merely signifies "original"; so $S/S_0 = 1.0$ represents the values used in the analysis whereas a ratio above 1.0 would indicate that actual stresses will be greater than those used in the analysis. The K_T value is a measure of the quality of the structure; it reflects holes, scratches, cut-outs, etc. A value of $K_T = 4.5$ is representative of the quality of aircraft structure generally sought during design, but as implied earlier, it's not unusual for K_T values to be as high as six or seven at some structural details.

It's noteworthy from both Figures (4.8.2-2 and 3) that a change of a few mph of cut-off wind speed, or a small change in either K_T or S/S_0 , can mean a change of very many years of life. Tests of structural details could significantly reduce the uncertainty of fatigue life prediction but were not considered cost-effective considering the experimental/demonstration nature of MOD-OA. Close monitoring of blade performance and condition will be provided.

4.8.2.2 LOW SPEED SHAFT

The low speed shaft diameter is set by the bearings that were selected. The critical stress point is the fillet on the rotor side of the downwind bearing. Based on nominal shaft diameter under normal operating conditions, the mean shaft stress is 2244 psi (15.5 MPa) and the alternating stress is 8057 psi (55.6 MPa). The fatigue strength of the 4340 steel shaft is a function of the fillet stress concentration factor, (K_T). The K_T value estimated for the shaft is 2.7 giving an endurance stress level of .19 times the ultimate stress of the shaft material. The ultimate is estimated at 105,000 psi (724 MPa) giving an allowable alternating stress of 19950 psi (138 MPa). Thus the shaft is adequate under normal operation. Off design and transient conditions, however, were not evaluated.

4.8.2.3 LOW SPEED SHAFT BEARINGS AND CAPS

The loads at the bearings are listed below. Bearing A is the upwind bearing

BEARING LOADS

BEARING	THRUST lbs (N)	VERTICAL lbs (N)	SIDE lbs (N)
A		9390 + 5796 (41,764 + 25,779)	3645 + 3243 (16,272 + 14,424)
B	3870 + 880 (17,212 + 3,914)	20856 + 8607 (92,760 + 38,281)	3423 + 2988 (15,224 + 13,290)

and bearing B, the downwind bearing. The bearings are Torrington No. 260SD32 which have a static load capacity of 670,000 lbs (3,000,000 N) and a dynamic capacity of 531,700 lbs (2,400,000 N) for 10^6 cycles. These bearings should have a near infinite life under the tabulated MOD-OA loadings.

A detailed analysis of the bearing caps was performed using a NASTRAN model. Under the tabulated loads, the maximum cap stress was calculated at 2400 ± 1500 psi (16.5 ± 10.3 MPa). The location is at a hole through the cap and the tabulated stress includes a stress concentration factor of three. At this stress level the bearing caps should also have near infinite life.

4.8.2.4 BEDPLATE

The bedplate was analyzed using a NASTRAN beam model. Section properties were determined for various portions of the bedplate length having nearly constant cross section. These section properties were used to define the properties of NASTRAN bar elements. Loads at the hub were applied in fifteen degree increments of blade azimuth angle. The stresses in the most highly stressed part of the bedplate are given in the following table.

BLADE AZIMUTH ANGLE, DEG	STRESS PSI	MPa	BLADE AZIMUTH ANGLE, DEG	STRESS PSI	MPa
0	5845	(40)	90	3177	(22)
15	7190	(50)	105	4271	(29)
30	7842	(54)	120	4743	(33)
45	7135	(49)	135	4066	(28)
60	5325	(37)	150	3752	(26)
75	3420	(24)	165	4464	(31)

The maximum stress occurs at a blade angle of thirty degrees and the minimum at ninety degrees. For fatigue analysis purposes, the stress variation becomes a static stress of 5510 psi (38 MPa) and a cyclic stress of 2333 psi (16 MPa).

The most highly stressed part of the bedplate occurs where the downwind section is welded to the center section. The AISC code was used to evaluate the fatigue resistance of this weld. It was determined that this was a Category C weld subjected to Loading Condition 4 (over 2×10^6). The allowable stress range is 12,000 psi (83 MPa). The bedplate cyclic stress is well within that required for infinite life. It should be noted that this weld was subjected to radiographic inspection; it could be uprated to Category B by grinding the weld flush or to Category A by grinding flush with the grinding in the direction of the applied stress. The allowable stress range for these categories is 15,000 psi (103 MPa) and 24,000 psi (165 MPa), respectively.

4.8.2.5 YAW DRIVE SYSTEM

The original design and fatigue analysis review of the MOD-0A wind turbine yaw drive system established two basic areas of concern. These areas of concern were:

1. Fatigue life in certain components.
2. Design for adverse environments, such as high temperature, sand storms, and salt laden atmosphere.

The utilization of the two yaw drive gear boxes as preloaded counter-acting brake systems was seen as an abnormal application of this hardware which would likely result in rapid deterioration of the yaw system. The use of bronze gears to react the high external load was seen as the greatest weakness of the system. The yaw drive assembly shaft couplings were also considered to be overloaded.

A yaw brake system acting in parallel with the gear drive system was recommended to keep external loads off of the gear boxes when the yaw drive is not functioning. This recommendation was accepted and a yaw brake was added to the system to react external nacelle yaw loads. This brake system limits yaw drive loads and decreases the number of load cycles applied to the yaw drive components. The lower surfaces of the yaw drive are exposed to the outside environment which includes sand storms and rain. Providing an environmental seal between the conical support and the base of the cylindrical housing was recommended.

4.8.2.6 TOWER

The tower was modeled for NASTRAN using bar (CBAR) and rod (CROD) elements. See Section 4.5.1 for discussion of the tower model. End fixity of bars was not relieved. Ninety rod elements and 144 bar elements were required to represent the structure. To ensure infinite life, the range of stress produced in each tower member by the operating loads was computed and compared⁶⁵ with the allowable fatigue stress ranges listed in Appendix B of the AISC Code.⁵²

Rated operating speed of the rotor is 40 rpm. Rotor-induced forces acting on the tower complete a cycle with each half revolution of the rotor. Therefore, less than 420 hours of rated operating time are required to generate two million loading cycles. It is necessary, then, to limit stress ranges to those values allowed for Loading Condition 4 (more than 2×10^6) of the AISC Code.

Seven allowable stress categories are listed under Loading Condition 4, with the admissible range of stress varying from 24,000 psi (165 MPa) for Category A to 6000 psi (41.4 MPa) for Category E. Selection of a particular category as the limiting design criteria is dependent upon the member type and fabrication details. For those tower elements with fillet-welded end connections, the minimum stress range of 6000 psi (41.4 MPa) is directly applicable. Most members, however, are not fillet welded and would be permitted a stress range greater than 6000 psi (41.4 MPa). It was not necessary to examine each tower element and connection detail for a differing stress range, the minimum allowable stress range of 6000 psi (41.4 MPa) was initially assumed applicable to all 234 elements of the tower model. The computer was instructed to output only those members whose computed range of stress exceeded 6000 psi (41.4 MPa). Those members so listed were then examined more closely for conformance with the Code.

The loads used in the analysis represent a relatively severe tower loading condition. This loading condition is expected to occur during operation of the

MOD-0A wind turbine near or at the maximum allowable wind velocity of 40 mph (18.0 m/s). The loads used for the NASTRAN static load subcases are shown in Table 4.8.2-5. Each subcase corresponds to one azimuthal position (fifteen degree increments of rotor angular position). Both forces and moments in the table were distributed equally to the four grid points (nodes) at the top of the tower. Both quasi-static and dynamic analyses of the tower were performed using the loads of Table 4.8.2-5. It was found that:

1. Both quasi-static and dynamic approaches give stresses which exhibit the same general profile.
2. One-percent damping has a negligible effect on the stress determined from the dynamic approach compared to that with no damping.
3. The stress determined from the quasi-static approach oscillates about a mean of 6000 psi (41.4 MPa) and has a range of about 5000 psi (34.5 MPa); that from the dynamic approach oscillates about a mean of 4300 psi (29.6 MPa) and has a range of 3000 psi (20.7 MPa).

This tends to indicate that the quasi-static approach is adequate though somewhat conservative. For that approach the minimum and maximum stresses in the rod members were -1610 and 1600 psi (-11.1 and 11.0 MPa), respectively. The minimum and maximum combined axial and bending stresses in the bar members were -8740 and 8780 psi (60.3 and 60.5 MPa), respectively. The maximum axial stress in all bar members was less than 2760 psi (19.0 MPa). Note the minimum and maximum stresses did not occur in the same member. Note also that these stresses are less than 50 percent of the static allowable stress, which is about 20,000 psi (138 MPa). The stress ranges were less than the fatigue stress allowable of 6000 psi (41.4 MPa). The stress ranges in the majority of the members of the tower were less than 3000 psi (20.7 MPa). The stress ranges were greater than 3000 psi (20.7 MPa) only in the horizontal members at the top of the tower and were mainly due to bending stresses near the end connections. It was concluded that the tower should have near infinite life.